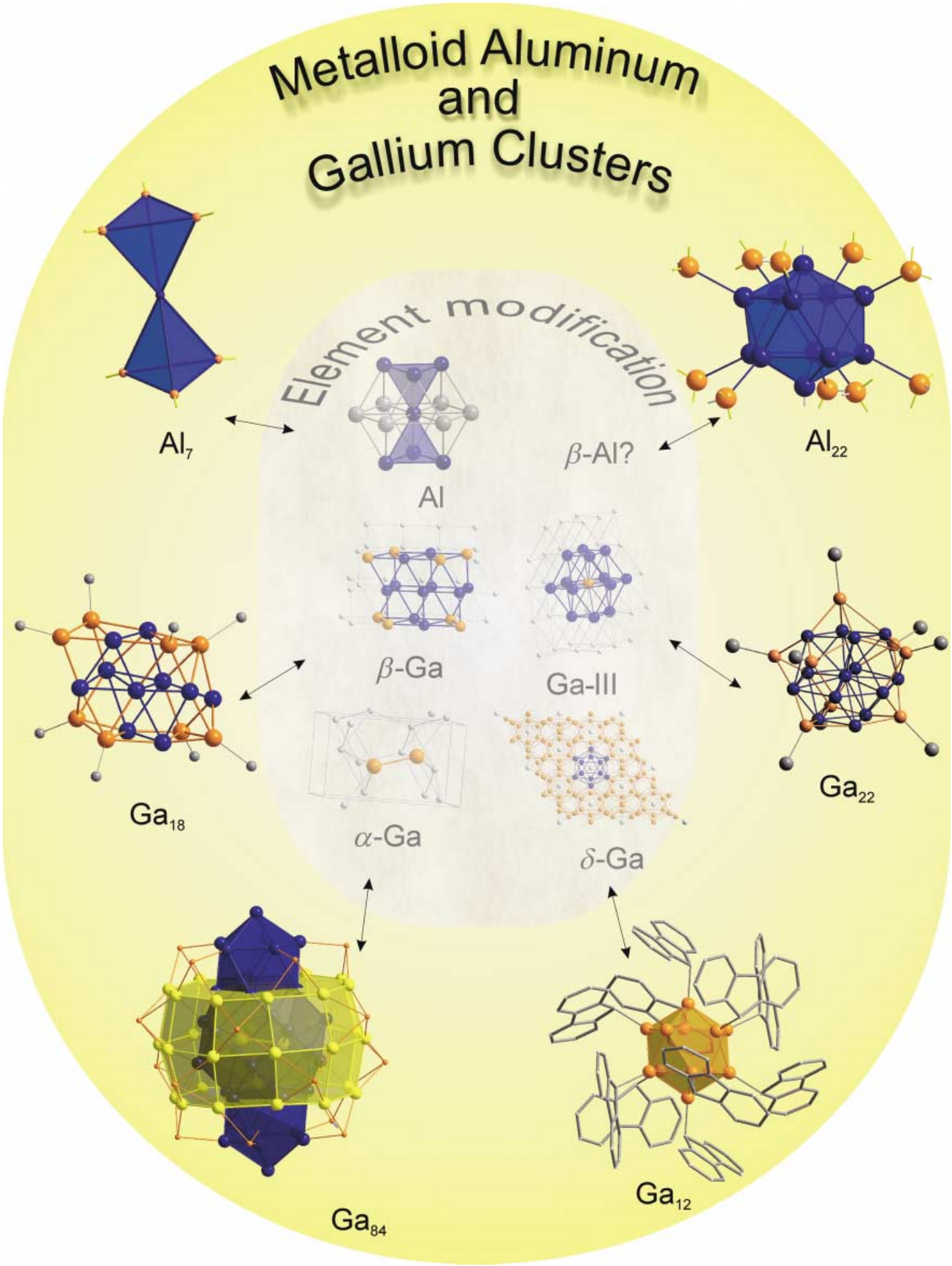

ANGEWANDTE CHEMIE

Metalloid Aluminum and Gallium Clusters: Element Modifications on the Molecular Scale?

Andreas Schnepf and Hansgeorg Schnöckel*

Dedicated to Professor Dieter Fenske on the occasion of his 60th birthday

As members of the same group in the periodic table, the industrially significant elements aluminum and gallium exhibit strong similarities in the majority of their compounds. In contrast there are significant differences in the structures of the two elemental forms: Aluminum forms a typical closest-packed metallic structure whereas gallium demonstrates a diversity of molecular bonding principles in its seven structural modifications. It can therefore be expected that differences between Al and Ga compounds will arise when, as for the elemental forms, many metal–metal bonds are formed. To synthesize such cluster compounds, we have developed the following synthesis procedure: Starting from gaseous monohalides at around 1000 °C, metastable solutions are generated from which the elements ultimately precipitate by means of a disproportionation reaction at room temperature. On the way to the elemental forms, molecular Al and Ga cluster compounds can be obtained by selection of suitable ligands (protecting groups), in which a core of Al or Ga atoms are protected from the formation of the solid element by a ligand shell. Since the arrangement of atoms in such clusters corresponds to that in the elements, we have designated these clusters as metalloid or elementoid. In accordance with the Greek word ειδος (ideal, prototype), the atomic arrangement in metalloid clusters represents the prototypic or ideal atomic arrangement in the elements at the molecular level. The largest clusters of this type contain 77 Al or 84 Ga atoms and have diameters of up to two nanometers. They hold the world record with respect to the naked metal-atom core for structurally characterized metalloid clusters.

Keywords: aluminum · cluster compounds · gallium · metal–metal interactions · structure elucidation

1. Introduction

Multi-atom, naked metal clusters are increasingly the subject of investigation by complex physical and quantum-chemical methods, for example, in nanotechnology[1, 2] because of their special properties in the transitional region between molecular and solid-state chemistry.[2] The interest in structure of such clusters is vividly illustrated by the 102 m high Atomium in Brussels, which represents an Fe_9 section from the structure of solid iron enlarged 150 billion times (Figure 1).

Figure 1. The Atomium in Brussels.

Clearly the creators of the Atomium assumed that an Fe_9 molecule would have the same structure as a section from the solid structure of iron, since they describe their design as an Fe_9 atomic molecule. However, as far as we are aware there is no experimental proof for the existence of such a structure of a molecular Fe_9 cluster. To obtain information on the arrangement of metal atoms in multiple-atom clusters, chemists have for many years been attempting to synthesize ligand-protected metal-atom clusters to compare their struc-

[*] Prof. Dr. H. Schnöckel, Dr. A. Schnepf
Institut für Anorganische Chemie
Universität Karlsruhe (TH)
Engesserstrasse, Geb.30.45, 76128 Karlsruhe (Germany)
Fax: (+49) 721-608-4854
E-mail: hansgeorg.schnoeckel@chemie.uni-karlsruhe.de

  1433-7851/02/4101-3533 $ 20.00+.50/0

ture and properties with that of the corresponding solid metal.[2]

We have described such clusters, which contain both ligand-bearing and naked metal atoms that are only bonded to other metal atoms, as *metalloid*,[3] to express, in accordance with the Greek word ειδος (ideal, prototype), that the ideal form or the motif of the solid structure can be recognized in the topology of the metal atoms in the cluster. The original limits of the term *metalloid*—used, for example, for the elements silicon and germanium which are metal-like with respect to certain macroscopic properties (e.g. metallic luster)—were extended to include the metalloid clusters, thus accessing an additional structural level, which was only possible through crystal structure analysis.

In general such metalloid clusters contain more direct metal–metal contacts than metal–ligand contacts. This means that metalloid clusters represent a sub-group of the extensive metal-atom cluster group in which, according to the definition of Cotton,[4] non-metal atoms may also be present.

Until a few years ago, metalloid clusters were known exclusively for the noble transition metals since these could be handled with relative ease (e.g. in aqueous solution). The $[Au_{55}(PPh_3)_{12}Cl_6]$ cluster[5] is the prototype of this family. Unfortunately no experimental structure data has been determined for this cluster since suitable crystals are not available.

The, at the time, largest metalloid noble-metal clusters to be structurally determined contain 6 naked Pt ($[Pt_6Ni_{38}CO_{48}H]^{5-}$),[6] 11 naked Pd ($[Pd_{59}(CO)_{32}(PMe_3)_{21}]$),[7] and—since 2000—55 naked Pd atoms with no ligand connections ($[Pd_{145}(CO)_{60}(PEt_3)_{30}]$; Figure 2).[8] Therefore it was very surprising when a metalloid cluster with 57 naked aluminum atoms ($[Al_{77}R_{20}]^{2-}$, $R = N(SiMe_3)_2$) was prepared and structurally determined in our group about five years ago (Figure 3).[9] This result was all the more surprising since the synthesis of the first molecular compound

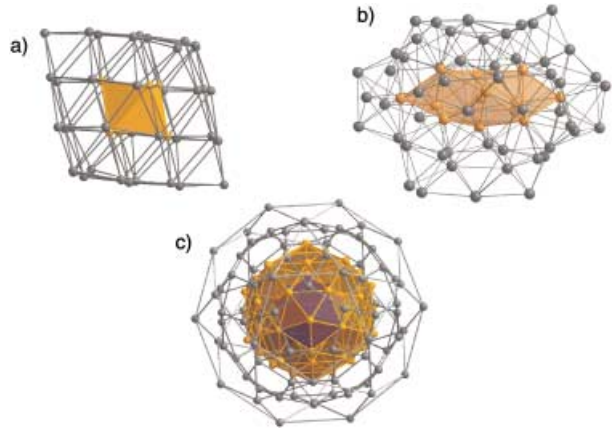

Figure 2. Molecular structure of the metalloid noble-metal clusters a) $[Pt_6Ni_{38}(CO)_{48}H]^{5-}$ b) $[Pd_{59}(CO)_{32}(PMe_3)_{21}]$, and c) $[Pd_{145}(CO)_{60}(PEt_3)_{30}]$. The naked metal atoms are highlighted in color.

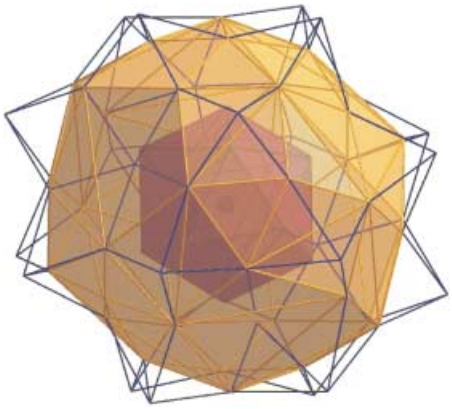

Figure 3. Layered representation of the arrangement of the 77 Al atoms [1 + 12(red) + 44(yellow) + 20(blue)] in the metalloid cluster $[Al_{77}\{N(SiMe_3)_2\}_{20}]^{2-}$ (**5**).

Hansgeorg Schnöckel, born in Marienburg, Western Prussia, studied chemistry at the University of Münster, where he also gained his doctorate under the supervision of H. J. Becher in 1970 on the spectroscopic investigations of boron-containing molecules. Subsequently he undertook matrix investigations of reactive high-temperature molecules, which formed the basis of his Habilitation in 1981. In 1987 he became professor of the University of Münster and in 1989 at the Institute of Inorganic Chemistry at the University of Munich. Since 1993 he has held the chair for analytical chemistry at the University of Karlsruhe. His research interests, that initially concentrated on the spectroscopic and quantum chemical investigations of reactive molecules, have in recent years shifted to synthetic chemistry of aluminum and gallium(I) halides and most recently to the synthesis of metalloid Al and Ga cluster compounds. The synthesis of such cluster units with dimensions on the nanometer scale and the investigation of the geometric and electronic structure by means of experimental and quantum-chemical methods are now central to his research activities with the aim of synthesizing and decomposing metalloid clusters as intermediates on the way from metal atoms to the bulk material.

H. Schnöckel

A. Schnepf

Andreas Schnepf, born 1968 in Karlsruhe, studied at the University of Karlsruhe, where he received his doctorate in 2000 with studies on polyhedra and metalloid clusters of gallium under the supervision of Professor Schnöckel. He is currently investigating subvalent compounds of the fourth main group of elements at the University of Karlsruhe.

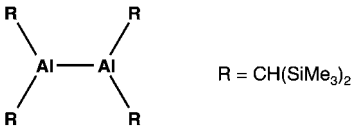

Figure 4. Schematic representation of the first diallane.

($[Al_2\{CH(SiMe_3)_2\}_4]$; Figure 4) with a 2 electron 2 center (2e2c) aluminum–aluminum bond had only been achieved in 1988.[10] In this case, and in many others, mainly smaller aluminum and gallium compounds were prepared, usually by traditional synthesis methods[11–14] (e.g.: dehalogenation reactions: $RMX_2 + Na$; or reactions with "GaI" originating from ultrasonic treatment[15]). Such methods will only be discussed in passing in this review.

We have developed another synthesis variant in which the gaseous monohalides, prepared at around 1000 °C, are subsequently isolated in metastable solutions at −78 °C.[16, 17] The halogen atoms are substituted by bulky groups and in a parallel disproportionation reaction (e.g. $3\,AlCl \rightarrow 2\,Al + AlCl_3$), large Al or Ga clusters are formed. Analogue to the above-mentioned Al_{77} cluster, we have also succeeded recently by such means to synthesize further metalloid aluminum and gallium clusters with diameters on the nanometer scale. In these cases the topology of the metal atoms in the clusters usually reflects that of the metal, or it can be used to give an indication of element modifications yet to be discovered.[16b,c, 23]

2. Synthesis of Metastable Aluminum- and Gallium-Halide Solutions

2.1. Principles and Experimental Details

The equilibrium between the liquid metal and gaseous mono- and trihalides is described for the example of aluminum [Eq (1)].

$$2\,Al_{(l)} + AlCl_{3(g)} \overset{1000\,^\circ C,\ 10^{-2}\ mbar}{\rightleftharpoons} 3\,AlCl_{(g)} \qquad (1)$$

The conditions for gallium are almost the same, with the exception that to achieve a comparable ratio of the partial pressures of mono- to trihalide the reaction temperature should be about 100 K lower.

In general, as a result of the increase in entropy, the equilibrium of this endothermic reaction shifts in favor of the gaseous monohalide with increasing temperature and with decreasing total pressure.[18] The transport of aluminum in the presence of $AlCl_3$ as described by Klemm et al. and later by Schäfer is also based on the reaction of Equation (1).[19] The partial-pressure behavior of the gaseous components is solely determined by the thermodynamic data of the mono- and trihalides and the molten metal, which means that it does not matter which halogenation medium is used in the preceding reaction. Thanks to its easy handling and to ensure a continuous stream of gaseous AlX (X = Cl, Br, I) we used a flow of the respective hydrogen-halide gas (e.g. HCl) at about 1000 °C over aluminum [Eq. (2)].

$$Al_{(l)} + HCl_{(g)} \rightleftarrows \tfrac{1}{2}H_2 + AlCl_{(g)} \qquad (2)$$

Under these conditions (ca. 10^{-1} mbar total pressure), for example, for the chloride system, there is a more than 20-fold excess of AlCl over $AlCl_3$.

To investigate the reactivity of molecular monohalides, we had previously carried out many matrix isolation experiments, which showed that AlX species preferentially oligomerize in solid argon. For example, a ring-shaped structure with D_{2h} point symmetry was inferred from the spectroscopic data for the dimeric species.[20, 16a] In addition to oligomerization, only the very first reaction and the most recent reaction from the matrix experiments will be mentioned here:

As far back as 1978 we were able to demonstrate the formation of the first threefold coordinate aluminum hydride halide ($HAlCl_2$) from HCl and AlCl,[21] and recently we were able elucidate the reaction between AlF and O_2 in solid argon.[22] AlF was generated at about 1000 °C by passing CF_3H, which was used instead of HF for ease of handling, over molten Al. In addition to an $FAlO_2$ peroxide with C_{2v} point symmetry, an unexpected $FAl(O_2)_2$ species with slightly distorted C_{2v} point symmetry was formed. The formation of such compounds ($FAl(O_2)_2$ has a triplet ground state!) is an indication that similar species could also be formed as primary products during the surface oxidation of metallic aluminum.

The positive results from the matrix experiments, which were started about 12 years ago, have enabled us to produce monohalides in gram amounts for synthesis purposes.[17] Although the experimental realization of this idea has been described many times,[16, 23] it will be presented briefly here because this experiment forms the basis for all the chemistry to follow. The required co-condensation apparatus is shown in Figure 5. At the center of a vacuum system of about 30-liter

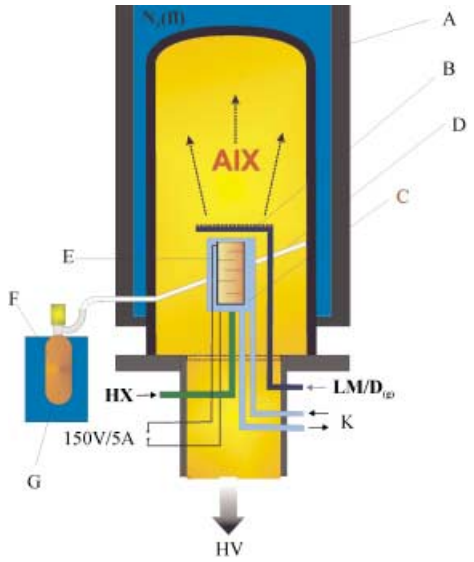

Figure 5. Scheme of the co-condensation apparatus: A = stainless steel vessel (30 L); B = solvent input (LM/D); C = Al in the graphite cell with resistance heating; D = drainage channel; E = cooling shield; F = Schlenk line; G = Dewar with dry ice (−78 °C); K = cooling water; HX = hydrogen halide gas; HV = high vacuum.

volume is a high-temperature reactor which contains molten aluminum at around 1000 °C in several graphite chambers. A flow of hydrogen-halide gas is directed through these reaction

chambers, and the flow is measured by means of the pressure drop in a storage vessel. In general about 40 mmol AlX is synthesized in two hours. After exiting the reactor the gaseous AlX molecules condense, without undergoing further collisions, on the cooled outer walls of the stainless steel vacuum vessel at $-196\,^{\circ}C$. To prevent the aggregation of the AlX species which disproportionate to form aluminum metal, that is, the reverse reaction in Equation (1), when warmed to above $-100\,^{\circ}C$, an excess of a suitable solvent must be co-condensed with the monohalide molecules. We generally use toluene to which a variable amount of a donor component has been added (e.g. NEt_3, Et_2O, THF). When the solid solvent mixture is melted at about $-100\,^{\circ}C$, deep red solutions are usually obtained which subsequently disproportionate according to Equation (1) in the temperature range -40 to $+50\,^{\circ}C$ depending on the halide and the donor and its concentration to the metal and the corresponding trihalide. The metastable AlX and GaX solutions are the starting points for the chemistry described in the following sections.

2.2. Limitations and Advantages of the AlX/GaX Synthesis Method

The limitations of the synthesis method described in Section 2.1 arise from the availability and capabilities of a precision mechanical workshop, since it requires the construction of high-vacuum apparatus in stainless steel involving many vacuum parts, and high- and low-temperature components. The optimization of our apparatus has continued over many years and with new information arising from almost every experiment the apparatus undergoes constant technical improvement. Despite the limitations of the method that mainly arise from the sensitivity and weaknesses of the apparatus, there are many advantages over classical procedures:

- Subvalent halides such as the ring-shaped Al_4X_4[24] and Ga_8X_8 species (Figure 6),[25] the first Al^I and Ga^I halides to be structurally investigated, are synthesized directly from the above-mentioned primary solutions; this is only possible by this method. The same applies to the first aluminum subhalides with a polyhedral Al framework: $Al_{22}X_{20}$ (X = Cl,[26] Br[27]). These Al_{22} compounds will be described in Section 3.2. Other halides and partially substituted halide compounds are the subject of a recently published review.[28]
- In the classical reduction of $RGaX_2$ compounds, for example, with reductants such as alkali metals, temperatures of 50 to $110\,^{\circ}C$ are generally applied which means that only GaR species that contain kinetically stable GaR bonds can be synthesized (e.g. GaCp*;[29] $Cp^* = C_5Me_5$): Metastable GaX solutions are so reactive that almost every metathesis reaction (e.g. with $LiN(SiMe_3)_2$) proceeds at temperatures above $-78\,^{\circ}C$. This means that our method can be used to obtain, for example, the unsubstituted compounds GaCp[30] and AlCp[31] ($Cp = C_5H_5$) in solution at low temperatures.
- Disproportionation reactions that proceed even under mild conditions (see above) can give rise to metalloid Al and Ga clusters that contain an increasing number of naked Al or Ga atoms with increasing reaction temperature. When applied to gallium chemistry the trisyl group ($C(SiMe_3)_3$) provides some impressive examples. The classical dehalogenation methods of Uhl et al. enabled the first tetrahedral Ga_4R_4 compound ($R = C(SiMe_3)_3$) to be synthesized[11], we succeeded in synthesizing a Ga_8 compound from a GaBr solution in toluene/THF at lower temperatures [32] in which tetrahedral Ga_4R_3 groups are connected over a Ga_2 unit (i.e. two naked Ga atoms (see Figure 19). At room temperature the same reaction yields a $Ga_{19}R_6$ cluster,[3] that contains 13 naked Ga atoms (see Figure 27), which demonstrates that the disproportionation reaction at this temperature proceeds much further along the path towards generating the metal. Both compounds will be discussed in more detail in Section 4.3.3 and 4.4.3.

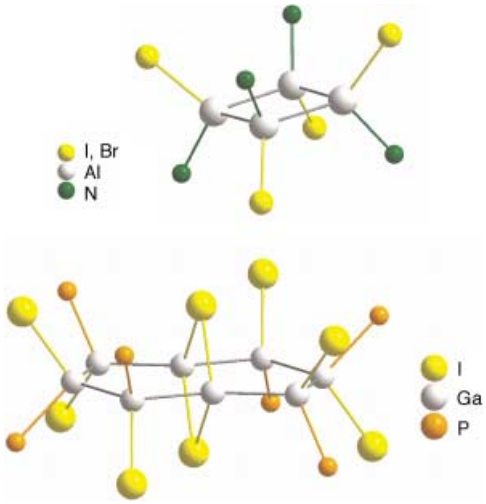

Figure 6. Molecular structures of binary halides $Al_4X_4 \cdot 4NEt_3$ (X = I, Br; top) and $Ga_8I_8 \cdot (PEt_3)_6$ (bottom). Of the donor molecules only those atoms directly bonded to the metal atoms are shown.

3. Aluminum Clusters

3.1. Metalloid Aluminum Compounds

After the first compound with a 2e2c Al–Al bond was synthesized by Uhl (Section 2.2)[10] and after we had synthesized AlCp*,[33] the first organo–Al^I compound, the objective was to synthesize metalloid aluminum-cluster compounds with as many naked Al atoms, that is, atoms with no attached ligands, as possible. The $N(SiMe_3)_2$ ligand proved to be a particularly favorable ligand in this endeavor since it was apparent that the substitution of the halogen atoms ($AlX + LiR \rightarrow LiX + AlR$) and the disproportionation of the AlX species ($3\,AlX \rightarrow 2\,Al + AlX_3$) occur in the same temperature range. Reactions in which substitution is favored tend to the formation of oligomeric AlR species (e.g. $(AlCp^*)_4$), whereas when substitution is hindered or when there is no suitable substituent the formation of aluminum metal through disproportionation of the AlX species is observed.

In the following section only metalloid aluminum clusters are discussed that are protected by an outer shell of the above-

mentioned $N(SiMe_3)_2$ ligand. These clusters therefore contain a naked Al_n core surrounded by $AlN(SiMe_3)_2$ groups with strong 2e2c Al–N bonding, in other words bonding between Group III/V elements.

The size of the Al_n cluster core is determined by the reactivity of the AlX solution with respect to disproportionation. Therefore, for a particular halide the size of the resulting cluster can be increased by an increase in temperature: Starting from an AlCl solution, for example, the cluster size progresses from an $[Al_7R_6]^-$ (**1**) cluster at $-7\,^\circ C$[34] through an $[Al_{12}R_6]^-$ (**2**) cluster[35] at room temperature through to an $[Al_{69}R_{18}]^{3-}$ (**4**) cluster after warming briefly to $60\,^\circ C$.[36] When, however, a less reactive AlI solution is used, at room temperature a partially substituted Al_{14} cluster **3** is obtained,[37] whereas after warming briefly to $60\,^\circ C$ the above-mentioned $[Al_{77}R_{20}]^{2-}$ (**5**) cluster[9] forms; in all cases R is the $N(SiMe_3)_2$ ligand. The cluster compounds **1**–**5** are extremely sensitive to moisture and air and may even spontaneously combust after only brief exposure to the atmosphere. Therefore handling these compounds for all physical measurements can be exceptionally difficult (see Section 4.4.6). This behavior contrasts dramatically with that of the metalloid noble-metal clusters (e.g. the Au_{55}[5] and Pd_{145} species[8]), some of which can be handled in aqueous solution and in contact with air. This difference is to be expected: it is comparable to the differences between the noble and the base metals.

All the above-mentioned metalloid Al clusters **1**–**5** form an Al_n cluster framework, which can be described as a distorted section from the structure of solid aluminum. The geometries of the Al_n frameworks of Al clusters **1**–**5** are shown in Figure 7a–e, whereby the distance between the center points of the Al atoms furthest apart increases from 5.46 to 13.35 Å in the series of Figures 7a →e.

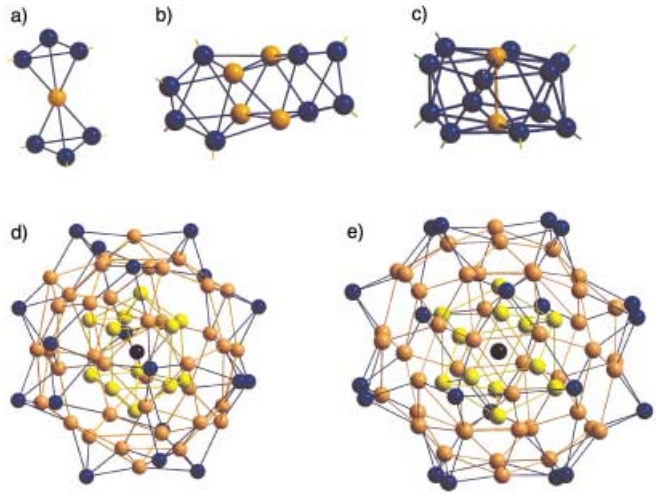

Figure 7. Geometrical arrangement of the Al atoms of the metalloid aluminum clusters: a) $[Al_7R_6]^-$ (**1**); b) $[Al_{12}R_6]^-$ (**2**); c) $[Al_{14}R_6I_6]^{2-}$ (**3**); d) $[Al_{69}R_{18}]^{3-}$ (**4**); e) $[Al_{77}R_{20}]^{2-}$ (**5**); $R = N(SiMe_3)_2$.

The description of these clusters as molecular nanostructured element modifications therefore appears plausible. This definition is further elucidated in Figure 8 which shows the topological relationship of clusters **1** and **2** to the structure of

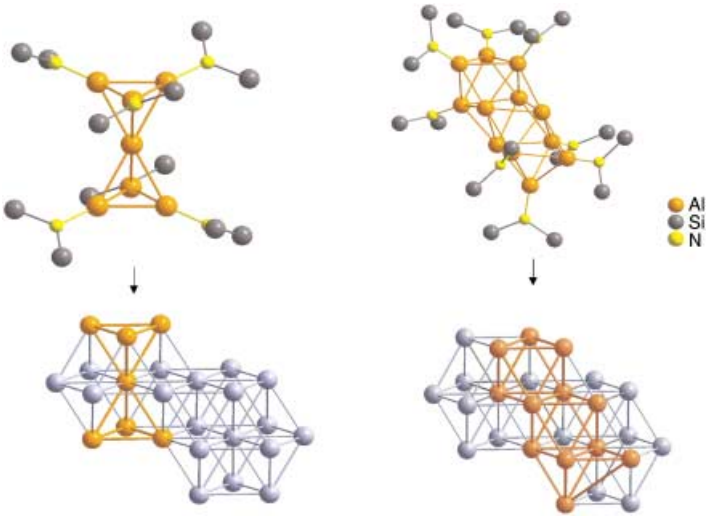

Figure 8. Molecular structures of the metalloid aluminum clusters $[Al_7R_6]^-$ (**1**; left) and $[Al_{12}R_6]^-$ (**2**; right) and the corresponding sections from the solid-state structure of elemental aluminum. $R = N(SiMe_3)_2$.

solid aluminum.[38] The metallic luster of crystals of clusters **4** and **5** is a further similarity to aluminum.

The relationship of the "wheel-rim-type" structure of the Al_{14} compound **3** to the metal can be demonstrated by a 30° rotation of the two centered Al_6 rings followed by a shift of the six-membered rings towards each other. The other possibility of the formation of an Al_{14} polyhedron with D_{6d} point symmetry by displacement of the naked central atom has been shown to be energetically unfavorable by quantum-chemical calculations: The observed metalloid structure is favored over the anticipated polyhedral structure[39] described by Wade.[67]

The principle and the significance of metalloid clusters for the understanding of the formation of metals are made clear by the two largest Al clusters **4** and **5** (Figure 7d, e) which are almost the same size with 69 and 77 Al atoms and 18 and 20 $N(SiMe_3)$ groups. In both cases a central Al atom is surrounded by 12 nearest neighbors. Despite the great similarity between the two clusters—the coordination number of the Al atoms decreases from the center to the periphery, the mean Al–Al distance decreases from the center to the periphery indicating that the Al–Al bonds have become more localized and have more molecular character from the inside to the outside—the coordination spheres of the central Al atoms are significantly different: The Al_{13} core of the Al_{69} cluster **4** can be described as distorted D_{5h} (this geometry is often described as decahedral[40]) whereas the central Al atom in the Al_{77} cluster **5** has been shown to have an icosahedral coordination sphere that is distorted in the direction of a cuboctahedron (Figure 9). Therefore both cases show a different geometry than for the noble-metal clusters: for example, for the Au_{55} cluster a cubooctahedral and icosahedral environment has been postulated and for the Pd_{55} framework of naked Pd atoms at the center of the Pd_{145} cluster an almost undistorted icosahedral Pd_{13} unit has been observed.[8] This situation demonstrates that for these large metalloid clusters (Al_{69} **4**,[36] Pd_{145},[8] Al_{77} **5**,[9] and a larger Ga_{84}

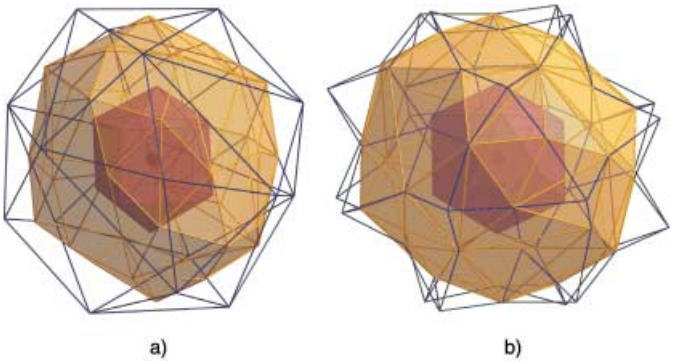

Figure 9. Arrangement of the Al atoms in the metalloid clusters a) $[Al_{69}R_{18}]^{3-}$ (**4**) and b) $[Al_{77}R_{20}]^{2-}$ (**5**) in a layered representation: **4** 1 + 12(red) + 38(yellow) + 18(blue) Al atoms; **5** 1 + 12(red) + 44(yellow) + 20(blue) Al atoms. $R = N(SiMe_3)_2$.

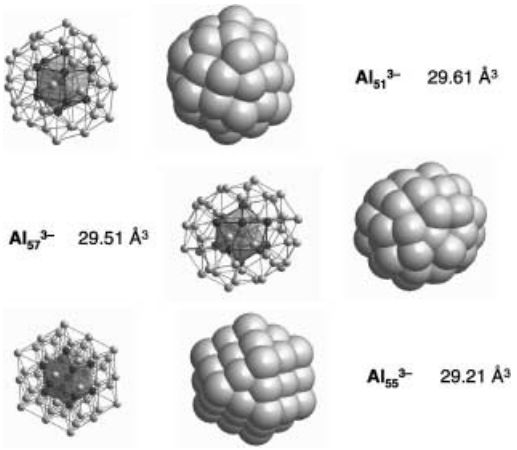

Figure 10. Arrangement of the naked Al atoms in $[Al_{69}R_{18}]^{3-}$ (**4**; section of the Al_{51}^{3-} structure) and $[Al_{77}R_{20}]^{2-}$ (**5**; Al_{57}^{3-} section), and an Al_{55} section from the solid-state structure of elemental aluminum in ball-and-stick and space-filling representations including the calculated mean atomic volumes for the Al atoms in these three clusters. $R = N(SiMe_3)_2$.

cluster **10**, which will be described in Section 4.4.6), for which structural data are available, there are significant differences in the centers both amongst the clusters themselves and to the corresponding metals, whereby the Pd_{145} cluster is the most similar with respect to the topology of the metal. However, in all cases the distance of the 12 nearest neighbors from the central atom is shorter than that in the metal, which shows that the bonding has shifted away from predominantly delocalized in the metal in the direction of localized molecular bonding.

We find the significant differences in the Al_{13} center of the Al_{69} cluster and the Al_{77} cluster frameworks of particular interest. Apparently even small changes in the cluster shell, which are probably too small to be observed with common nanoscopic methods (e.g. AFM: atomic force microscopy), lead to changes in the topology of the metal framework at the center which then affect the electronic properties. Unfortunately apart from a preliminary band-structure calculation of the Al_{77} cluster[41] there have been no detailed investigations that could lead to a deeper understanding of the interactions between the cluster shell and the core. Such investigations, which could make use of the experimental structural data, could serve to model metal-surface reactions, such as the dissolution of aluminum. The structures of **4** and **5** suggest that $Al^{I}R$ units are formed primarily on the surface. According to the observations of **4** and **5**, such primary reactions could also lead to changes in the interior of the metal, even in the nanometer range.

To approach an understanding of the relationship between the structures of the Al_{69} and Al_{77} clusters and that of metallic aluminum, we have compared frameworks of 51 and 57 naked Al atoms from these two clusters with an Al_{55} unit from the metal. To do this, single-point self-consistent-field (SCF) calculations were carried out based on the experimental data from all three species[36] and the volume enclosing an area of the same electron density (0.004 e Å; Figure 10). The results showed that the mean atomic volume (volume of the Al_n cluster framework/number of Al atoms) decreases in the order $Al_{51}^{3-} > Al_{57}^{3-} > Al_{55}^{3-}$. For improved comparability the same charge of 3 − , was specified. Although the Al–Al bonds of the Al_{55} cluster were the longest (2.86 Å, as in Al metal) the increase in the coordination numbers in the order $Al_{51}^{3-} < Al_{57}^{3-} < Al_{55}^{3-}$ leads to a contraction of the Al_n cluster framework. The stepwise disproportionation of Al^{I} compounds, which always yields Al metal at temperatures above around 60 °C, is therefore associated with a contraction of the metal atom framework. This conclusion suggests that a closer investigation of the precipitates with metallic luster that are sometimes observed to form metallic mirrors on the vessel walls after disproportionation would be worthwhile. These could be larger Al clusters with cores of Al atoms that have contracted even further in the direction of the metal.

All previously discussed metalloid Al clusters show that the favored arrangement of Al atoms is a closest packing as in the metal, whereby the observed distortions reflect the adaptation of the cluster core to the AlR "corset". Since the packing density comes ever closer to that of the metal with increasing cluster size (Figure 10), it is conceivable that there is an alternative pathway during the early stages of cluster formation that could lead to a less compact modification of aluminum. This hypothesis may not be so unlikely since the other Group III metals, boron and gallium (see Section 4), also exist in several modifications. An experimental indication for a hypothetical β-aluminum modification is given by the results discussed in the following Section 3.2.

3.2. Al_{22} Clusters as Intermediates in the Formation of Hypothetical β-Aluminum

Directly after the condensation of AlX species, for example, in the presence of strong donors, the donor-stabilized $Al_4Br_4 \cdot 4NEt_3$ compound[24] is obtained in which the bonding can be described by means of classical 2e2c bonds (see Section 2.2). With weaker donors such as THF, the first polyhedral Al subhalides $Al_{22}X_{20} \cdot 12L$ (X = Br (**6**),[27] Cl (**7**),[26] L = THF, tetrahydropyran (THP)) with a unique structure were recently obtained (Figure 11). The icosahedral Al_{12} core of **6** and

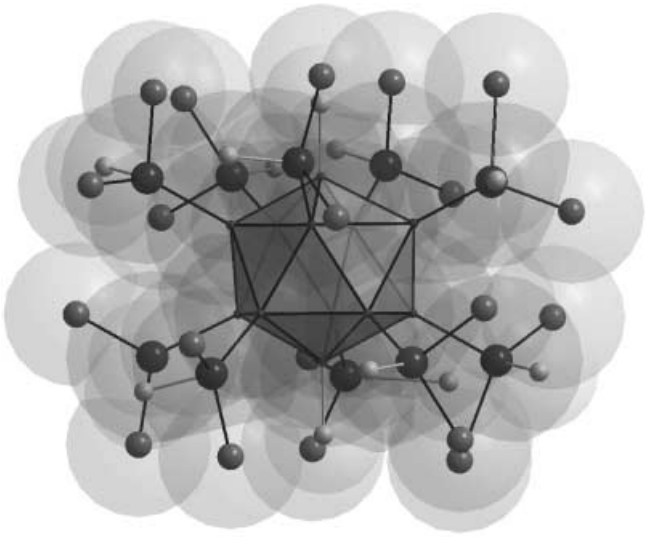

Figure 11. Molecular structure of $Al_{22}Br_{20} \cdot 12\,THF$ (**6**). Of the THF molecules only the O atoms directly bonded to the Al atoms are shown.

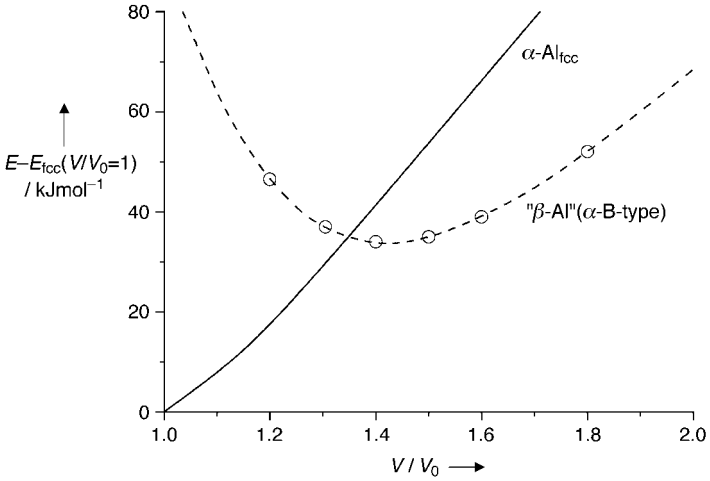

Figure 12. Calculated energy pathway for the real (—— α-Al) and hypothetical (– – – β-Al) aluminum solid-state modifications during expansion.

7 is reminiscent of the polyhedral boron subhalides (such as B_4X_4, B_8X_8, B_9X_9, and $B_{12}X_{12}^{2-}$),[42] in which each halogen atom X is directly bonded to a boron atom of the polyhedral framework. In contrast, in the Al_{22} halides **6** and **7**, ten more Al atoms are directly bonded each to an Al atom of the icosahedral Al_{12} framework to present a unique configuration. The outer ten Al atoms are additionally bonded each to two halogen atoms and saturated by a donor molecule. The apex and base atoms in the Al_{12} icosahedron are naked, that is, they are each only shielded by one donor molecule. This type of metal-atom topology is surprising because it has not been observed for any element. It could be expected for boron clusters since, for example, the α-boron modification[43] in which a network of molecular icosahedral cluster units are to some extent connected by boron–boron bonds. Despite the great sensitivity of these Al_{22} subhalides, it was possible to obtain solid-state ^{27}Al NMR and X-ray photoelectron spectroscopy (XPS) measurements, which showed indeed that three electronically different types of Al atoms are present.[26, 44]

With respect to the bonding of the Al atoms the structure of these $Al_{22}X_{20}$ clusters shows some similarity to bonding in β-rhombohedral boron (which contains a B_{84} unit with a central icosahedral B_{12} framework of which all the boron atoms are connected to B_6 units[27]). Therefore, ab initio calculations were carried out on the stability of a hypothetical Al modification with the structure of α-boron.[26] The calculations show that with an expansion of the closest-packed Al atoms in aluminum metal by about 30% a structure analogous to α-boron would be energetically more stable (Figure 12). An expansion of this type would be associated with an energy consumption of about 33 kJ mol^{-1}. As was shown in the discussion of the Al_{69} and Al_{77} clusters (**4** and **5**; Figure 7d, e), a contraction in the direction of the bulk-metal structure does take place during disproportionation, thus the intermediate existence of a β-Al modification with a larger atom volume cannot be excluded. This hypothesis is supported by model calculations that reveal that intermediate compounds analogous to **6** and **7** could be synthesized during disproportionation of $AlCl \cdot H_2O$ to $Al_{(solid)}$ and $AlCl_3$, that could then react further via a hypothetical β-Al modification to the final products $Al_{(solid)}$ and $AlCl_3$ (Figure 13).[26, 27]

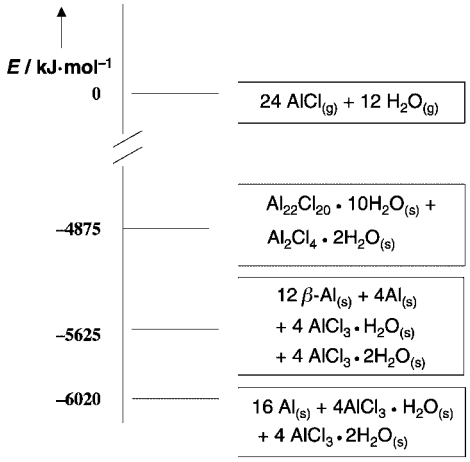

Figure 13. Calculated energy scheme for the modeled disproportionation of AlCl to Al and $AlCl_3$ in the presence of H_2O as the donor.

For gallium, its wide range of structures containing molecular units will be discussed in Section 4,[23] the most recent calculations performed in an analogous fashion predict that a previously unknown modification with the α-boron structure could be much easier to obtain since the required energy input during expansion is only about 20% of that required for Al.[84]

To summarize it can be stated that metalloid Al clusters which form structures with a constant ligand shell ($N(SiMe_3)_2$) show a close similarity with the topology of crystalline aluminum. The size of the clusters, which are intermediates on the way to the bulk metal, can be increased by increasing the temperature, however, temperatures above about 60 °C lead exclusively to the metal. It is possible that there is

another reaction pathway which would lead initially to a polyhedral $Al_{22}X_{20}$ cluster. There are many indications that this cluster can be regarded as an intermediate on the way to a new hypothetical Al modification.

4. Metalloid Gallium Compounds

4.1. The Modifications of the Element

The structurally demonstrated existence of seven modifications for elemental gallium gives rise to the expectation of a larger diversity of metalloid clusters than observed for aluminum, for which only one element modification is known. To classify the topologies of the Ga atoms in all the Ga clusters described below, the most prominent structural features of the seven modifications are described in the following section. In Figure 14 the structural units typical of the normal-pressure modifications α-,[45] β-,[46] γ-,[47] and δ-gallium[48] and for the high-pressure modifications Ga-II and Ga-III[49] are shown. Recently under very high pressure a Ga-IV modification was detected which has a fcc packing of the Ga atoms.[49b]

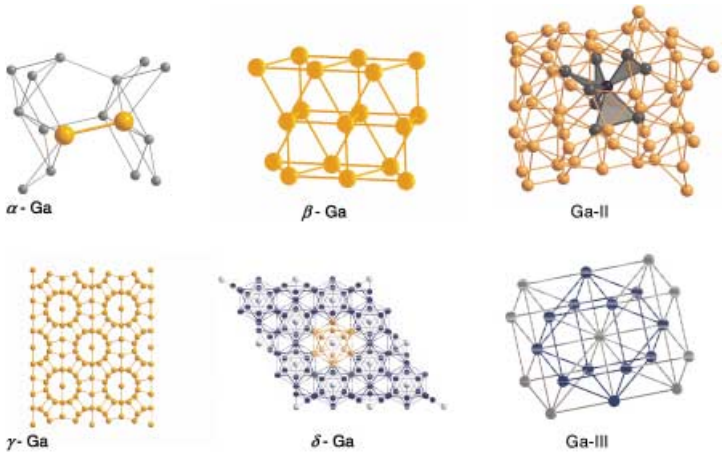

Figure 14. Sections of the normal-pressure solid-state modifications α-, β-, γ-, and δ-gallium and the high-pressure modifications Ga-II and Ga-III.

For α-gallium (coordination number 1+2+2+2) the short Ga–Ga bond of 2.45 Å is characteristic, so that α-gallium is also described as a molecular metal made up of Ga_2 dumbbells. For the low-temperature phases β-, γ-, and δ-gallium the following characteristic units are observed: the ladder structure (coordination number 2+2+2+2) for β-gallium, Ga_7-rings that stack to form tubes and a centered Ga_n "wire" observed for γ-gallium, and connected Ga_{12} icosahedra for δ-gallium. In all cases pseudomolecular gallium units can be discerned that indicate a degree of covalent bonding, and therefore similarity to the neighboring element boron. In contrast, in the three high-pressure modifications Ga-II, Ga-III, and Ga-IV high coordination numbers and topologies of Ga atoms are observed (Figure 14) that point to analogies with the packing schemes of "true" metals such as the neighboring element aluminum.[49, 50]

The diversity of bonding options for Ga atoms to each other that are apparent from the different modifications can also be observed in the metalloid clusters. These metalloid clusters could also be described, perhaps more suitably and comprehensively, as *elementoid* clusters since the atomic topologies observed are similar to those found in the bulk element. The special features of gallium in comparison to boron and aluminum in the elemental state, indicate that it would be less than helpful to describe the metal-rich compounds of all three elements on the basis of a single rule even though all three have the same number of valence electrons. The lack of a single ordering principle is a shortcoming, particularly for the gallium clusters, since as a result of their improved synthesis procedures, there is a larger number of them than the corresponding aluminum clusters. A purely formal means of classification for the gallium clusters would be to take, in addition to the oxidation number, the number of gallium atoms to demonstrate analogies to the topologies of the elemental state in the corresponding element modification.[51]

4.2. Gallium – Gallium Bonds

Before starting the discussion of metalloid gallium clusters with several Ga–Ga bonds, it would be appropriate to make a few basic remarks on gallium – gallium bonding and a critical comment on gallium – gallium triple bonds: A molecular organometallic compound containing the first Ga–Ga 2e2c bond[52] was synthesized by Uhl et al. at the end of the 1980s (Figure 15 a).[53] To clarify the term metal – metal bond, we

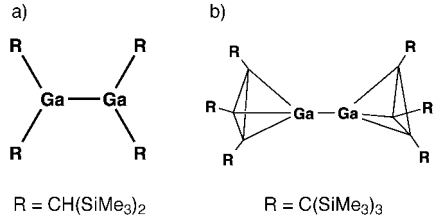

Figure 15. Schematic representation a) of the first digallane and b) $[Ga_8\{C(SiMe_3)_3\}_6]$ (**9**).

have designated the $[Ga_8R_6]$ cluster ($R = C(SiMe_3)_3$; Figure 15 b, and Figure 19), mentioned in Section 2.2, as a prototypic compound[32] with a 2e2c metal – metal bond, this is because each of the atoms participating in the Ga–Ga bond does so without bridging atoms and is exclusively bonded to other metal atoms of the same type. With the help of quantum-chemical calculations on the model compounds $[Ga_2H_4]$ and $[Ga_4H_4]$ and the experimental data for $[Ga_2R_4]$ and $[Ga_4R_4]$ the strength of the metal – metal bond in $[Ga_8R_6]$ can be classified as lying between that of a classical 2e2c bond and a 2e3c bond.[59] Such bonding found in cluster elements (e.g. in fullerenes and Zintl ions) is currently of intense interest and a review article on this topic has recently appeared.[54]

Although there are no indications for the existence of Ga–Ga double bonds, a discussion regarding the "Ga–Ga triple bond" has raged for several years.[55] This was initiated

by a remarkable experimental result in which a compound (**11**) with a $[Ga_2R_2]^{2-}$ unit (R = 2,6-$C_6H_3Trip_2$; Trip = 2,4,6-$C_6H_2iPr_3$)[56] and bridging Na^+ ions was investigated structurally and with the aid of quantum-chemical calculations.[57] As a result of the short Ga–Ga bond length (2.32 Å) the term Ga–Ga triple bond was introduced for this bond. Critical assessments of the interpretation of the bonding in the $[Ga_2R_2]^{2-}$ unit were to be anticipated as there are other examples of short Ga–Ga bonds for which it is unlikely that a triple bond is present, for example, a) the Ga–Ga bonds of 2.35 Å in digallane [{GaN(Dipp)CH = CH(Dipp)}$_2$] (Dipp = 2,6-diisopropylphenyl),[58] b) the Ga_2 dumbbell discussed in Section 4.4.6 (d(Ga–Ga) = 2.35 Å) in the Ga_{84} cluster **10**, and c) the above-mentioned Ga_2 unit in α-Ga, which despite a coordination number of seven for each Ga atom, exhibits an unexpectedly short bond of 2.45 Å. We also consider the description "triple bond" to be at least misleading since, if the term is used literally, a bond should hold together atoms and therefore a triple bond should be characterized by triple bond strength in comparison to a single bond. Since the bonding strength is graphically illustrated by the restoring forces during bond stretching, the force constant provides a good measure and shows that the Ga–Ga "triple bond" can at best be described as a strong single bond.[59] It is apparent that the six electrons contributing to the bond strength do so to very different extents. In contrast the force constants for the corresponding bonds with arsenic (the next-but-one neighbor to gallium) yield the anticipated trend, that is, a ratio of 1:1.9:3.1 for the force constants of single, double, and triple bonds in the model compounds As_2H_4, As_2H_2, and As_2.[59]

In addition to the force constant, there are other indications that the short distance of the Ga–Ga "triple bond" is significantly influenced by the bridging Na^+ ions, so that in **11** we may in fact be dealing with a [RGaNa$_2$GaR] cluster (Figure 16a).[60] To avoid the use of, in our opinion, a misleading definition of multiple bonds for the heavier main-group elements, we proposed an alternative description: 4e2c bonds instead of double bonds and 6e2c bonds instead of triple bonds.[60, 61]

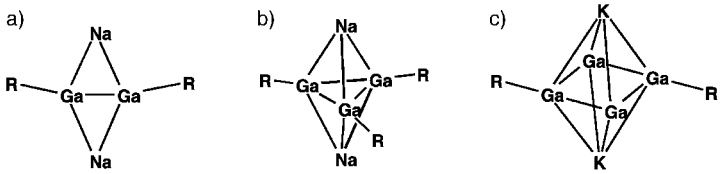

Figure 16. Schematic representation of the compounds a) $[Ga_2R_2Na_2]$ (**11**, R = 2,6-$C_6H_3Trip_2$) b) $[Ga_3R_3Na_2]$ (**12**, R = 2,6-$C_6H_3Mes_2$), and c) $[Ga_4R_2K_2]$ (**13**, R = 2,6-$C_6H_3Trip_2$).

4.3. Ga_n Clusters ($n = 4$ to 9)

A central motif in quite a few gallium clusters is the Ga_2 unit (e.g. $[Ga_6R_8]^{2-}$ (**8**), $[Ga_8R_6]$ (**9**), and $[Ga_{84}R_{20}]^{4-}$ (**10**)), which is a defining structural feature for α-gallium (see Section 4.1). Of note is that in the $[Ga_2R_2Na_2]$ species **11**[56] (see Section 4.1; Figure 16a), the Ga_2 unit has the oxidation state 0 which means that the reduction has already proceeded to the elemental state. Therefore this Ga_2 unit (or a $[Ga_2Na_2]^{2+}$ cluster) lies on the borderline between the Zintl anions on the one side[104] and the metalloid gallium clusters with their intermediate oxidation states between +1 and 0 on the other. A similar analysis leads from the $[Ga_3R_3Na_2]$ species (**12**; R = 2,6-$C_6H_3Mes_2$; Mes = 2,4,6-$C_6H_2Me_3$)[62] to the $[Ga_3Na_2]^{3+}$ units[63] or from the $[Ga_4R_2K_2]$ compound (**13**; Figure 16c R = 2,6-$C_6H_3Trip_2$) [64] to the $[Ga_4K_2]^{2+}$ and $[Ga_4{}^0]$ clusters.[105] Since the Ga–Na and Ga–K bond lengths in all the clusters of this type lie in the ranges anticipated from the sum of the metal radii, an assessment with the help of additional quantum-chemical calculations[65] should lead to a deeper understanding of the bonding in these Ga clusters that goes beyond the merely descriptive use of the term Ga–Ga multiple bonds.[60]

4.3.1. Ga_4 and Ga_5 Clusters

$[Ga_4R_4]$ species[11, 66] with a tetrahedral Ga_4 framework represent the starting point in gallium-cluster chemistry. As in the corresponding $[Al_4R_4]$ species, these clusters should be designated as pre-*closo* clusters according to the Wade–Mingos rules[67, 93] and not metalloid clusters because they contain exclusively ligand-bearing Ga atoms. Despite this, the Ga_4 cluster in the $[Ga_4R_2K_2]$ species **13** (Figure 16c) has interesting bonding with respect to metalloid properties since the formal oxidation state of the Ga atoms is 0. The short Ga–Ga bonds of 2.46 Å and the planarity of the Ga_4 units point to analogies to both α-gallium (Ga–Ga = 2.45 Å) and β-gallium with its ladder structure. A $[Ga_4R_4Na_2]$ compound (R = Si*t*Bu$_3$)[68] can be described as an intermediate between the tetrahedral $[Ga_4R_4]$ cluster and the formally neutral planar Ga_4 unit in $[Ga_4R_2K_2]$, as it contains a butterfly-type Ga_4 framework and the oxidation state 0.5 (Figure 17b). Two other Ga_4 clusters with intermediate oxidation states of +1 and +1.5 have a Ga_4 framework with (distorted) D_{3h} point

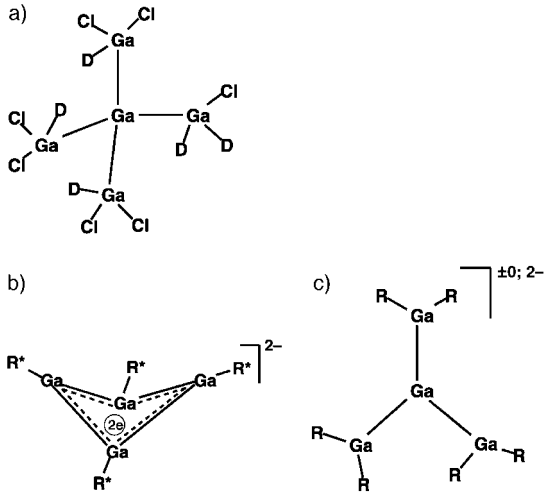

Figure 17. Schematic representation of the compounds a) $[Ga_5Cl_7(Et_2O)_5]$, b) $[Ga_4(Si*t*Bu_3)_4Na_2]$, c) $[Ga(GaR_2)_3]$ (**14**), and $[Ga(GaR_2)_3Na_2]$ (**15**). R = Trip.

symmetry: $[Ga(GaR_2)_3Na_2]$ (**14**; R = Trip)[69] and $[Ga(GaR_2)_3]$ (**15**; R = Trip; Figure 17c).[69] The central naked Ga atoms to which the formal oxidation state 0 can be assigned are a step in the direction of metalloid clusters.

A description similar to that of the latter Ga_4 clusters can also be applied to a Ga_5X_7 halide,[70] in which a naked Ga atom (also formally Ga^0) is surrounded tetrahedrally by four Ga atoms. Three of the surrounding Ga atoms are attached to two halogen atoms whereas the fourth gallium atom is only attached to one halogen atom (Figure 17a). An analogous Al_5X_7 compound with a similar structure was recently synthesized (a halide transfer leads to the crystalline compound via two ionic species $[Al_5X_8]^-$ and $[Al_5X_8]^+$).[71]

4.3.2. Ga_6 Clusters

We recently reported on the $[Ga_6R_8]^{2-}$ cluster compound (**8**, R = $SiPh_2Me$; Figure 18)[72] in which the mean oxidation state of the gallium atoms is +1. After removal of two R^- groups the formation of an octahedral $[Ga_6R_6]$ pre-*closo* unit,

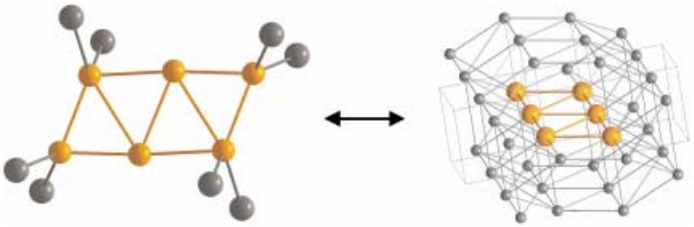

Figure 18. Molecular structure of $[Ga_6(SiPh_2Me)_8]^{2-}$ (**8** omitting Ph and Me groups) and the corresponding section from the solid-state structure of β-gallium.

analogue to the tetrahedral $[Ga_4R_4]$ cluster mentioned in Section 4.3.1, could be assumed. Model calculations have shown, however, that a rhomboid Ga_6 unit with two naked Ga atoms would be favored over the pre-*closo* cluster.[72] Similar calculations for the corresponding B_6 and Al_6 compounds—for which the octahedral units are favored—show that the Ga_6 cluster **8** is a special case. The similarity of the arrangement of the gallium atoms in **8** to that in β-gallium shows that, in contrast to aluminum and boron, specific connectivity principles predetermined by the element will be favored. The absence of a Ga_6 compound with an octahedral Ga_6 framework—in $[Ga_6Cp^*_6]$[29] the very long Ga–Ga bond lengths (4.07 and 4.17 Å) show that these bonds must described differently—and that many compounds with octahedral boron (e.g. $B_6I_6^{2-}$[73]) or Al_6 frameworks ($[Al_6R_6]^-$, R = *t*Bu[74]) exist, indicate that the topological similarities in certain element modifications and clusters are a result of the special bonding options available to gallium atoms. The description of the $[Ga_6R_8]^{2-}$ cluster **8** as *metalloid*—or in this case preferably as *elementoid* (in relation to β-gallium)–is therefore plausible.

4.3.3. Ga_8 and Ga_9 Clusters

The octameric GaI compound $[Ga_8I_8(PEt_3)_6]$ (Figure 6),[25] the first Ga_8 cluster, has already been mentioned. The oxidation state of the Ga atoms of +1 and the classical 2e2c Ga–Ga bonds confirm that this cluster cannot be described as metalloid. The Ga_8 cluster $[Ga_8R_6]$ (**9**; R = $C(SiMe_3)_3$) is a model compound for a 2e2c metal–metal bond (Section 4.2).[32] This cluster (Figure 19) can be described as

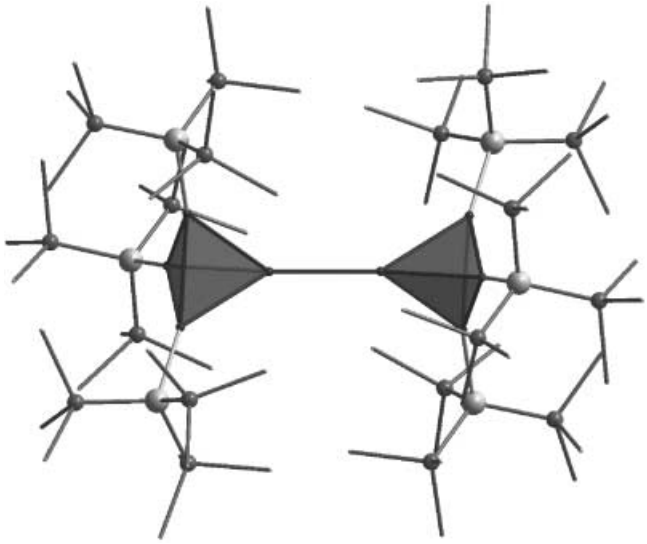

Figure 19. Molecular structure of $[Ga_8\{C(SiMe_3)_3\}_6]$ (**9**).

metalloid for two reasons: firstly the central Ga_2 unit reflects the motif of α-gallium. Secondly the Ga_2 unit with a distance of 2.61 Å between the Ga atoms can be described as a link in the chain of the Ga_n wire in the center of the Ga_7 tubes of γ-gallium (Ga–Ga 2.60 Å; see Figure 14). A $[Ga_8R_6]$ cluster (**16**; R = supersilyl = Si*t*Bu$_3$) recently synthesized by Wiberg et al. shows a completely different geometry.[75, 76] The Ga cluster framework in **16** is illustrated together with the that of the analogous $[Ga_8R_6Na_2]$ species **17** (R = supersilyl) in Figure 20.

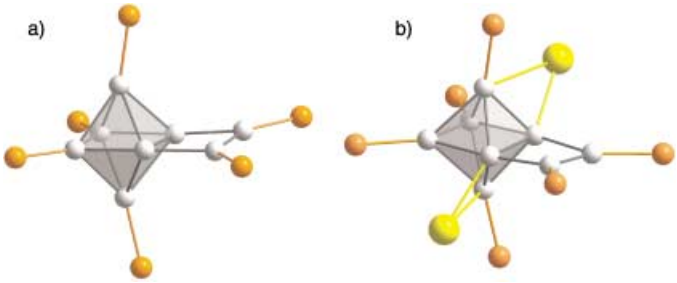

Figure 20. Molecular structures of a) $[Ga_8R_6]$ (**16**) and b) $[Ga_8R_6]^{2-}$ (**17**) omitting the *t*Bu groups. R = Si*t*Bu$_3$.

Wiberg et al. showed that the unexpected Ga_8R_6 framework (Ga_6R_4 with linking Ga_2R_2 groups) in **16** can be described with the help of the Wade–Mingos rules as a twofold capped tetrahedrotetragallane (hypo-pre-*closo*-hexagallane; $2n-2$ cluster electrons) and the $Ga_8R_6^{2-}$ unit in **17** ($2n+2=$ 14 cluster electrons) as a *closo* compound in which the two neighboring R groups can be replaced by the RGaGaR group.[75] It is also evident that the planar Ga_6 unit in **16** and **17**, in particular because of the presence of two naked Ga atoms, bears a similarity to that in the above-mentioned $[Ga_6R_8]^{2-}$ cluster **8** (Figure 18), which is also described as

metalloid. The oxidation state of 0.75 in **16** and 0.5 in **17** in contrast to +1 for **8** shows, however, that reduction has already proceeded extensively in the direction of a three-dimensional connectivity of the gallium atoms as found in elemental gallium (in this case β-gallium). For **17**, the Ga–Na bonds of almost 3.00 Å (also approximately the sum of the metal radii) indicate that the sodium atoms,[65] have to be included as part of the cluster framework (see discussion in Section 4.2). Such interactions between lithium atoms and a gallium-cluster framework can generally be excluded since in all previous cases the lithium ions are completely screened from the cluster anion by coordinating donor molecules. In Section 4.4 the relationship between the $[Ga_8R_6]$ clusters **16** and **17**, and the $[Ga_{10}R_6]$ and $[Ga_{18}R_8]$ clusters **22** and **27** will be discussed.

The dianion $[Ga_8R_8]^{2-}$ (**18**; R = fluorenyl) has a square-antiprismic framework of eight Ga atoms and has eight σ bonds to the fluorenyl ligands (Figure 21).[77] According to

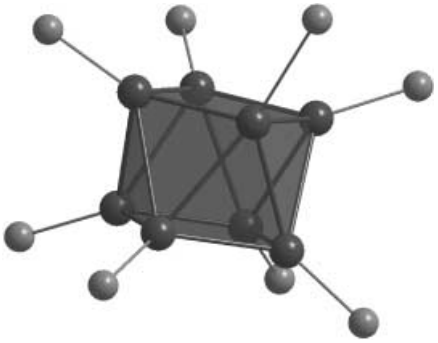

Figure 21. Molecular structure of $[Ga_8(C_{13}H_9)_8]^{2-}$ (**18**). Of the fluorenyl ligands only the C atoms directly bonded to the Ga atoms are shown.

the Wade–Mingos rules, such a cluster with $2n+2$ framework electrons should form a dodecahedral (Do) *closo* cluster. The square-antiprismic (SA) form actually observed could also be plausibly explained with the help of DFT calculations on the model compounds $[Ga_8H_8]^{2-}$ and $[B_8H_8]^{2-}$ (each with Do and SA structures). The results showed that the experimentally determined SA form of $[Ga_8H_8]^{2-}$ is indeed the most favorable (8 kJ mol^{-1}), whereas for $[B_8H_8]^{2-}$ as anticipated the Do form is energetically favored (62 kJ mol^{-1}). Since the sequence of orbitals for the two $[Ga_8H_8]^{2-}$ isomers do not differ much from each other **18** should be described as a *closo* compound despite the basic square-antiprismic form.[77] Compound **18** clearly differs from the second compound with fluorenyl as the ligand $[Ga_{12}R_{10}]^{2-}$ (**21**; R = fluorenyl), which will be discussed in Section 4.4.1.

The $[Ga_9R_9]$ cluster (**19**; R = *t*Bu, Figure 22)[78] recently synthesized by Uhl et al. can also be described as a threefold capped prism, a pre-*closo* gallane, which demonstrates clearly the analogy to the corresponding $B_9X_9^{n-}$ compounds (X = H, halogen; $n = 0-2$).[79] A mean oxidation state of 0.56 for the Ga atoms in the $[Ga_9R_6]^-$ cluster (**20**; R = $Si(SiMe_3)_3$; Figure 22b)[80] synthesized in 1997 by Linti from "GaI" points to a metalloid structural element (see Section 4.4.6 for the icosahedral-capped Ga_{84} cluster **10**; δ-Ga; Figure 14). On the

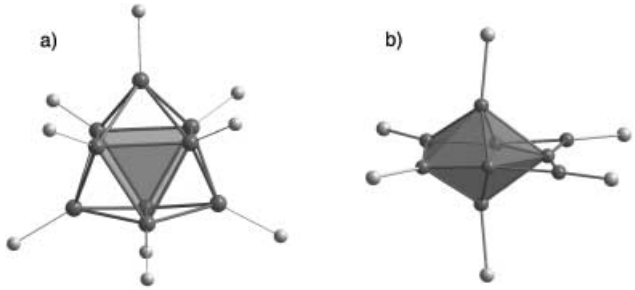

Figure 22. Schematic representation of a) $[Ga_9tBu_9]$ (**19**) and b) $[Ga_9R_6]^-$ (**20**; R = $Si(SiMe_3)_3$). Of the ligands only the C or Si atoms directly bonded to the Ga atoms are shown.

other hand this cluster with its $n-1$ total electron pairs does fit into the Wade–Rudolf–Mingos concept.[67]

The structural diversity of the Ga_8 and Ga_9 clusters shows the possibilities for variation in the connectivity of Ga atoms and the associated difficulty in describing and classifying the Ga_n clusters. On the other hand this diversity makes the investigation of gallium compounds so interesting since unexpected experimental findings may well form the basis for new bonding concepts. Particularly the larger Ga_n clusters, described in Section 4.4, can be described as molecular intermediates on the way to one of the seven gallium modifications. We will concentrate on this aspect since quantum-chemical calculations (including band-structure calculations) are possible in principle but have previously only helped in understanding the topology in individual cases. First formulations from this analysis method, which can be extended to band-structure investigations of hypothetical element modifications, could be developed to become the basis for a deeper understanding of these clusters as intermediates on the way to three-dimensionally ordered bulk material (see Section 4.4.1[84]).

4.4. Metalloid Ga_n Clusters ($n = 10-84$)

With an increasing number of Ga atoms and particularly with an increasing number of naked gallium atoms that bear no ligands, it is expected that the atomic configuration in the cluster will approach that of the element modifications, which means that metalloid or–often more appropriate–elementoid Ga clusters with mean oxidation states for the Ga atoms decreasing from +1 to 0 will result. Since there are obviously no strict limits for the total number of gallium atoms in the metalloid topology–Section 4.3 described metalloid partial structures for several smaller Ga clusters–in this section we will start with a Ga_{12} cluster for which the distorted icosahedral Ga_{12} unit is reminiscent of analogous *closo*-type compounds discussed in the Section 4.4.1, such as, **18**.[77] In Section 4.4.2 a Ga_{10} and a Ga_{13} cluster will be discussed in which the concept of the quantum-chemical calculated packing density and the experimentally accessible density variations in the element modifications, as mentioned for the Al_n clusters, plays a role. The $[Ga_{13}(GaR)_6]^-$ structure in the Ga_{19} cluster (Section 4.4.3) provides conclusive evidence for a better understanding of the bonding in the gallium-rich

clusters with 18, 22, and 26 Ga atoms (Section 4.4.4 and 4.4.5). Finally in Section 4.4.6 the bonding, structure, and some considerations of the physical properties of the $[Ga_{84}R_{20}]^{4-}$ cluster **10** will be given. With respect to the number of naked metal atoms, this cluster is the largest structurally characterized metalloid cluster.

4.4.1. Ga_{12} Clusters

There is no gallium cluster corresponding to the icosahedral $[Al_{12}R_{12}]^{2-}$cluster (R = *i*Bu),[81] with which Uhl et al. made a signification contribution to the renaissance of aluminum research. However, the $[Ga_{12}R_{10}]^{2-}$ cluster (**21**, R = fluorenyl),[82] is structurally similar. This cluster is formed together with the above-mentioned $[Ga_8R_8]^{2-}$ cluster **18** during the reaction of GaBr with fluorenyl lithium (Figure 23). Quantum-chemical calculations show that, in contrast to the model

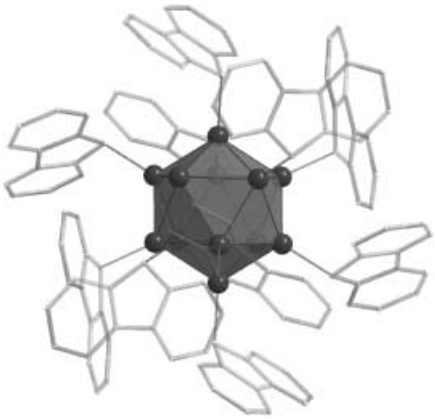

Figure 23. Molecular structure of $[Ga_{12}(C_{13}H_9)_{10}]^{2-}$ (**21**).

compound $[Al_{12}H_{10}]^{2-}$, the HOMO in a $[Ga_{12}H_{10}]^{2-}$ cluster is at a particularly unfavorable level for oxidation to the $[Ga_{12}H_{12}]^{2-}$ species so that the absence of a corresponding $[Ga_{12}R_{12}]^{2-}$ cluster appears to be plausible. On the other hand for aluminum the metalloid $[Al_{12}R_8]^-$ cluster **2** (analogous to $[In_{12}R_8]$[83]) exists in which a section from the close packing of metallic aluminum is realized. Apparently the formation of a similar structure for a Ga_{12} cluster is not favorable although the cleavage of two R^- groups from the cluster ($[Ga_{12}R_{10}]^{2-} \rightarrow [Ga_{12}R_8] + 2R^-$) should be possible. The absence of a normal-pressure modification with close-packed Ga atoms (in contrast to close-packed elemental structures of aluminum and indium) on the one hand and the realization of the δ-modification for gallium with its connected Ga_{12} icosahedra on the other, makes the formation of an icosahedrally distorted $[Ga_{12}R_{10}]^{2-}$ cluster plausible. From this viewpoint the designation metalloid for this cluster is reasonable. The reaction to yield the Ga_{84} cluster **10** (see Section 4.4.6), which also contains icosahedral partial structures with its $GaGa_5$ caps, also produced other clusters with structural units that were previously typical only for the element boron. The similarity of many Ga cluster compounds to the basic icosahedral framework in α-boron yields the first experimental indications that, in addition to the δ-modification, there may be a hypothetical modification for gallium that resembles α-boron. The most recent quantum-chemical band-structure calculations from Häussermann et al.,[84] based on the original work from von Schnering, Nesper, and Parinello et al,[50] show that this new phase should be much easier to realize than the β-aluminum phase (postulated in Section 3.2) and that our method of disproportionation under mild conditions (-50 to $+50\,^{\circ}C$) could enable possible experimental access to this new gallium modification.

4.4.2. Ga_{10} and Ga_{13} Clusters

Recently the clusters $[Ga_{10}R_6]$ (**23**; R = Si*t*Bu$_3$), $[Ga_{10}R_6]^-$ (**22**; R = Si(SiMe$_3$)$_3$), and $[Ga_{13}R_6]^-$ (**24**; R = Si*t*Bu$_3$), were synthesized by Linti and Wiberg et al.[85] The two Ga_{10} clusters **22** and **23** show differing topologies of the gallium frameworks (Figure 24). In the neutral cluster **22** there are two different

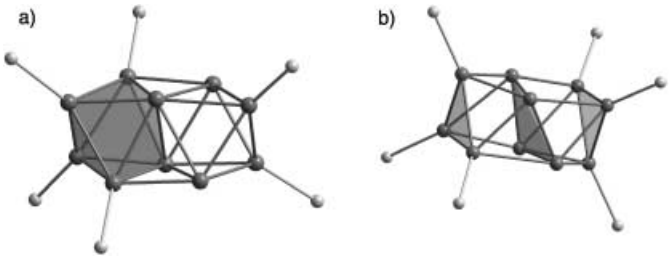

Figure 24. Molecular structures of a) $[Ga_{10}R_6]$ (**23**; R = Si*t*Bu$_3$) and b) $[Ga_{10}R_6]^-$ (**22**; R = Si(SiMe$_3$)$_3$). Of the ligands only the Si atoms directly bonded to the Ga atoms are shown.

octahedra (with two or four ligand-bearing Ga atoms, respectively) connected by a shared edge. In the cluster anion **23** two triangular faces of ligand-bearing Ga atoms—$(GaR)_3$–are connected over a rhomboid Ga_4 group. Since both Ga_{10} clusters contain the same number of ligands as the Ga_{13} cluster and in the case of **22** and **24** even the same type of ligand (Si*t*Bu$_3$), a detailed comparison of the structures would appear to be appropriate. Unfortunately the structural data for **24** were only rudimentary so that they could not be included in a database. However, we were able recently to synthesize $[Ga_7(GaR)_6]^-$ (**24′**; R = Si(SiMe$_3$)$_3$) which is related to **24** and to determine its structure (Figure 25).[86] The seven naked Ga atoms in **24′** form a cube which is missing a corner. The three complete square faces of the cube are capped with GaR groups. The three incomplete square faces are shielded by a $(GaR)_3$ group, with the center of the Ga_3 group pointing towards the missing corner of the cube. This arrangement is reminiscent of the structure of a $SiAl_{14}$ cluster (Figure 26),[87] in which a central Si atom is surrounded by a cube of naked Al atoms, the faces of which are each capped by AlR groups (R = Cp*).[88]

To determine the atomic volume of the Ga_n framework of the Ga_{10} and Ga_{13} clusters and thereby trace the progress of the formation of metal, we have carried out single-point SCF calculations, in analogy to the Al clusters (see Section 3.1 and Figure 10), for the anions **23** and **24′**, both containing six hypersilyl ligands ($Si(SiMe_3)_3$). As anticipated the atomic volume decreases from the Ga_{10} cluster (36.9 Å^3 per Ga atom)

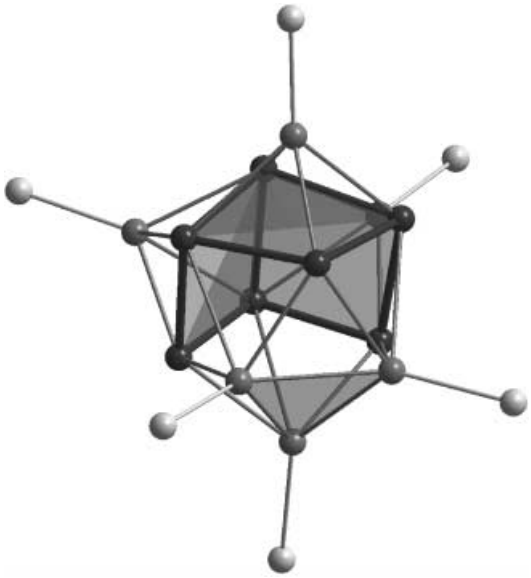

Figure 25. Molecular structure of $[Ga_{13}R_6]^-$ (**24′**; $R = Si(SiMe_3)_3$). Of the $Si(SiMe_3)_3$ groups, only the Si atoms directly bonded to the Ga atoms are shown.

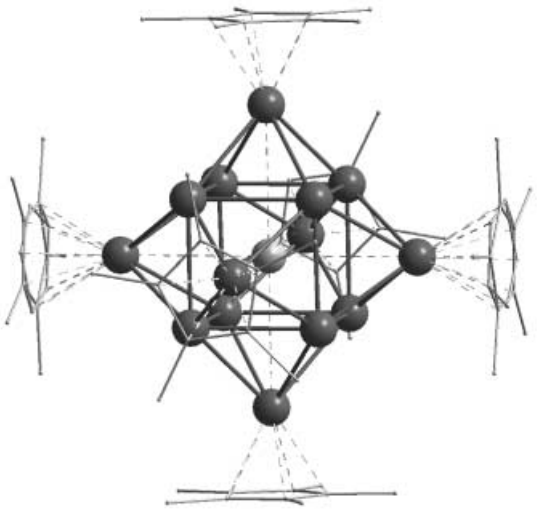

Figure 26. Molecular structure of the metalloid cluster $[SiAl_8(AlCp^*)_6]$.

to the Ga_{13} cluster (35.0 Å^3 per Ga atom) by around 5%. Since in neither case is there a centered structure, in contrast to $[Ga_{22}R_8]$ and $[Ga_{26}R_8]^{2-}$–clusters **26** and **28** (see Section 4.4.4), and since the ratio of the naked to the ligand-bearing Ga atoms is still low (0.66 for **23** and 1.17 for **24′**; in contrast to 1.75 for **26** and 2.2 for **28**) the mean atomic volumes for **23** and **24′** are still about 10% larger than those of the Ga_{22} and Ga_{26} cluster units. Further quantum-chemical calculations are required (e.g. separate calculations for the entire cluster and for the cluster core of naked Ga atoms), to compare, for example, the electronic structure (e.g. the HOMO/LUMO separation) with the results from the band-structure calculations for the real element modifications. To summarize it can be concluded that for **23** and **24′** with the same shell of six GaR groups a larger number of naked gallium atoms in the core of **24′** leads to a higher density and therefore a closer resemblance to the bulk material. This principle will become more apparent in Section 4.4.4 for clusters with a larger shell of eight GaR groups.

4.4.3. Ga_{19} Clusters

The $[Ga_{19}R_6]^-$ cluster (**25**; $R = C(SiMe_3)_3$); Figure 27)[3] under discussion here is remarkable for many reasons:

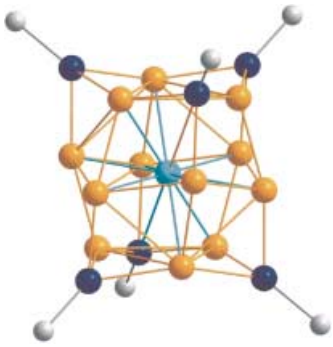

Figure 27. Molecular structure of $[Ga_{19}R_6]^-$ (**25**; $R = C(SiMe_3)_3$). Of the $C(SiMe_3)_3$ groups, only the C atoms directly bonded to the Ga atoms are shown.

- Cluster **25** is the only metalloid gallium cluster for which a ^{71}Ga NMR spectrum in solution has been obtained.
- **25** is a centered cluster in which the central gallium atom has the coordination number 12 the same as has in "real" metals.
- **25** is the only metalloid gallium cluster and, to our knowledge, the largest metalloid cluster for which MALDI and ESI mass spectra have been obtained,[89, 90] which provide for the first time experimental evidence about the bonding in such clusters.

The highly symmetrical environment of the central gallium atom enables the observation of the ^{71}Ga NMR signal at $\delta^{71}Ga = -134$ ppm[3] which is the only experimental evidence available for the assignment of calculated NMR spectrum chemical shifts to metalloid clusters: for example, $[Ga_{13}(GaR)_6]^-$: $R = H$, CH_3, $C(SiH_3)_3$; $\delta^{71}Ga = -6$, -109, -231 ppm. The results obtained show that the shifts calculated by the DFT method for naked Ga clusters–for example $[Ga_{13}]^-$ (I_h): $\delta^{71}Ga = -603$[3] and $[Ga_{13}]^-$ (D_{5h}): $\delta^{71}Ga = -455$[89]–differ drastically from those of ligand-shielded Ga clusters,[1, 3] and that conclusions from the results obtained for naked metal clusters can only be applied to ligand-shielded metalloid clusters to a very limited extent.

Application of the Jellium model to the cluster core of 13 gallium atoms gives rise, with 40 electrons, to the expectation of particularly high stability and therefore the observation of the $[Ga_{13}]^-$ ion in the mass spectrometric (MALDI) investigation as by far the most intensive peak was not surprising.[89] Investigations currently being performed with the ESIMS method have yielded the first indications[90] that collisions with inert-gas molecules remove sequentially the six GaR groups from **25** to finally result in the stable $[Ga_{13}]^-$ cluster as also observed in the MALDI experiments. The stability of this cluster anion is made more obvious by the

calculated value for the electron affinity of the neutral $[Ga_{13}]$ cluster. The value of 3.35 eV[89] corresponds approximately to that of the fluorine atom (3.45 eV). The stability of the $[Ga_{13}]^-$ cluster ion, which clearly illustrates the electron deficiency in clusters of the elements of the third main group and which is confirmed by the formation of Ga_n Zintl ions[104] also illustrates the difficulties that can be anticipated for any investigation on the reactivity of such Ga_{13} anions in the gas phase. In addition the great sensitivity of the $[Ga_{19}R_6]^-$ solution demands a large experimental effort to transfer the educt without it decomposing to the mass spectrometer and then to use the $[Ga_{13}]^-$ species obtained after fragmentation for further reactions in the gas phase. To summarize it can be stated that **25** represents a stroke of luck for the assessment of the bonding in Ga_n clusters, since it is possible for the first time to show unambiguously by experiment that GaR groups and not R^- groups can be designated as the shell of this cluster, and that for the first time for a central metal atom in a cluster an experimental value for the chemical shift in the NMR spectrum can be obtained.

4.4.4. Ga_{18}, Ga_{22}, and Ga_{26} Clusters

After two neutral compounds with the composition $[Ga_{22}R_8]$ (R = $Si(SiMe_3)$,[91] $Ge(SiMe_3)$[92]) had been obtained, we recently succeeded in synthesizing another representative of this type with supersilyl ligands, $[Ga_{22}(SitBu_3)_8]$ (**26**; Figure 28b).[93] Slight modification of the synthesis conditions

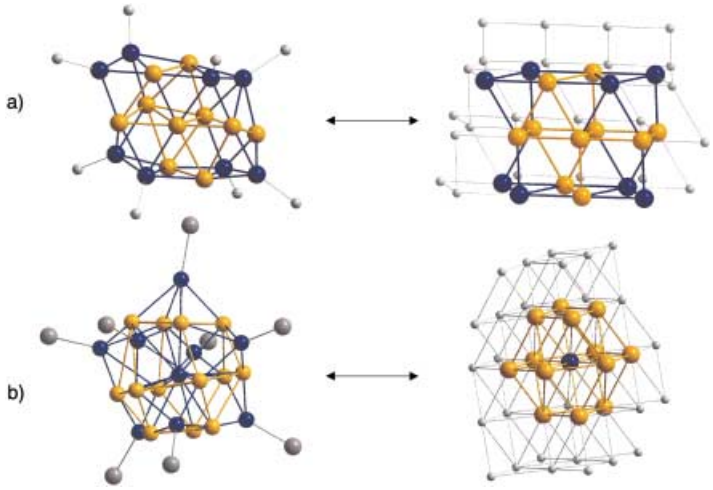

Figure 28. Molecular structures of a) $[Ga_{18}(SitBu_3)_8]$(**27**) and b) $[Ga_{22}(SitBu_3)_8]$ (**26**, of the $SitBu_3$ groups, only the Si atoms directly bonded to the Ga atoms are shown) and corresponding sections from the solid-state structures of β-gallium and Ga-III.

enabled a further neutral cluster to be obtained; the $[Ga_{18}R_8]$ cluster (**27**; R = $SitBu_3$; Figure 28a).[93] Analogous to the results for the Ga_{10}, Ga_{13}, and Ga_{19} clusters, **27** and **26** can be described as $[Ga_{10}(GaR)_8]$ and $[Ga_{14}(GaR)_8]$, which means that inside a cage of eight GaR groups are either 10 or 14 naked Ga atoms. For **26** a higher packing density and a smaller mean atomic volume is to be expected than for **27**. The above-mentioned single-point SCF calculations indeed showed that the mean atomic volume decreases from **27** to **26** by about 5%. As a result of the topological similarity of **27** to β-gallium and that of **26** to high-pressure modification gallium-(III) (Figure 28) it is not surprising that the experimentally determined density increases by about 5% between these two gallium modifications. Although in **26** and **27** there are a different number of naked metal atoms they are surrounded by the same number and type of ligands, thus making such comparisons plausible.

Since the supersilyl group ($SitBu_3$) is obviously somewhat bulkier than the hypersilyl group ($Si(SiMe_3)_3$), eight $GaSitBu_3$ groups lead to a cluster pair with 18 or 22 gallium atoms, whereas eight $GaSi(SiMe_3)_3$ ligands lead to a pair with 22 or 26 gallium atoms. The latter type of compound $[Ga_{18}(GaR)_8]^{2-}$ (**28**) was synthesized by Linti and Rodig from "GaI" in the form of black crystals that show metal luster in reflected light (Figure 29).[94] The cluster core in **28** is

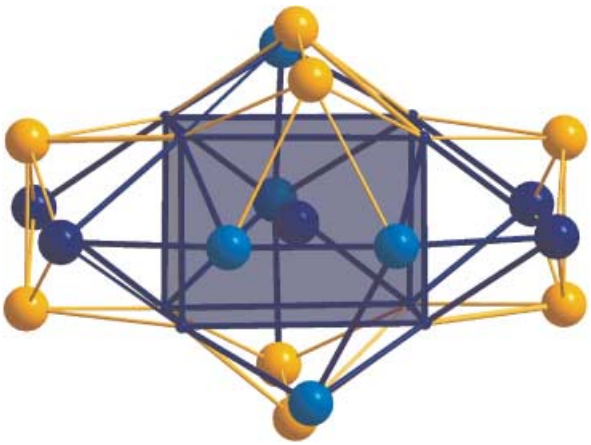

Figure 29. Arrangement of the 26 Ga atoms in $[Ga_{26}R_8]^{2-}$ (**28**; R = $Si(SiMe_3)_3$). The first coordination sphere around the central Ga atom is shown as a polyhedral representation and the Ga atoms attached to a ligand are orange.

particularly reminiscent of the high-pressure modification Ga-III with its 4+8 coordination. The Ga_{18} unit in **28** can be described as follows: A central gallium atom is surrounded by a pseudo cuboctahedron of 13 gallium atoms (8+3+2). The remaining four naked gallium atoms are part of two Ga_4R_2 units that are located over two Ga_4 faces of the Ga_{14} core.

To analyze the bonding situation, for most of the cluster compounds described here, physical measurements (e.g. UV/Vis, conductivity etc.) are required in addition to the successful structure investigation. As the investigations discussed later on in Section 4.4.6 the largest metalloid gallium cluster $[Ga_{84}R_{20}]^{4-}$ (**10**; R = $N(SiMe_3)_2$) shows, many surprises could be expected that could help to understand the special bonding in metalloid clusters as intermediates on the way to the bulk phase. Unfortunately, apart from the cluster compounds **10** (Ga_{84}) and **25** (Ga_{19}), great difficulties are to be expected because of a) the extreme sensitivity to air and moisture, b) the small crystal dimensions, and c) the reproducible but not yet optimized syntheses, resulting in insufficient yield.

4.4.5. Other Ga_{22} Clusters

Since it was possible to obtain the Ga_{22} cluster discussed in Section 4.4.4 with three different ligands, it is apparent that this electronic configuration is particularly stable. We assigned this to, amongst other factors, the closed Jellium configuration with 58 electrons ($14 \times 3 + 8 \times 2$).[91] Recently we were able to isolate another Ga_{22} compound for which this stability criterion also applies, but in which despite the same mean oxidation state of the gallium atoms a different arrangement of the 22 gallium atoms is observed: The use of "slender" $N(SiMe_3)_2$ ligands means that ten instead of eight ligands can fit in the outer shell so that a $[Ga_{22}R_{10}]^{2-}$ cluster ($R = N(SiMe_3)_2$) **29** results. The shell construction $GaGa_{11}(GaR)_{10}$ of **29** can be seen in Figure 30.[95]

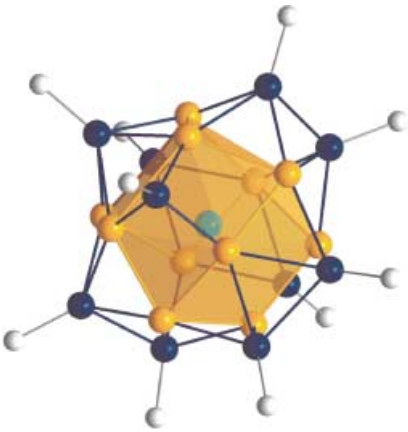

Figure 30. Molecular structure of $[Ga_{22}R_{10}]^{2-}$ (**29**; $R = N(SiMe_3)_2$; only the N atoms directly bonded to the Ga atoms are shown). The first coordination sphere around the central Ga atom is shown in a polyhedral representation.

Single-point calculations for the Ga_{22} cluster cores of **29** and **26** show that in the transition from **29** to **26** the atomic volume in the Ga_{22} unit decreases by 2%. We have interpreted this shrinkage in volume to mean that **29** can be considered an intermediate on the way from the β-modification (2+6 coordination) to the high-pressure Ga-III modification (4+8 coordination). This "phase transition" of a Ga_{22} unit is associated with an energy increase of 9 kJ (calculated from single-point SCF calculations). Analogously it was also determined that the high-pressure fcc gallium phase Ga-IV, is only a few kJ higher in energy, than the β-gallium modification.[50] Further calculations and experiments (e.g. UV/Vis spectra) are required to understand the relationship between such "nanostructured" phase transitions at the molecular level and true phase transitions in the bulk phase.

In addition the significance of the bulkiness of the ligands for the structure of the Ga_{22} clusters **29** and **26** and for the electronic properties of a cluster becomes clear. A hypothetical $[Ga_{22}R_9]^-$ cluster, which could result from the $[Ga_{19}R_6]^-$ cluster **25** discussed in Section 4.4.3 by the addition of three GaR groups, should stabilize, depending on the bulkiness of the ligand, by elimination of a R^- group (large ligand) or by addition of another R^- ligand (small ligand) to yield $[Ga_{22}R_8]$ or $[Ga_{22}R_{10}]^{2-}$; clusters analogous to **26** and **29** (Figure 31).

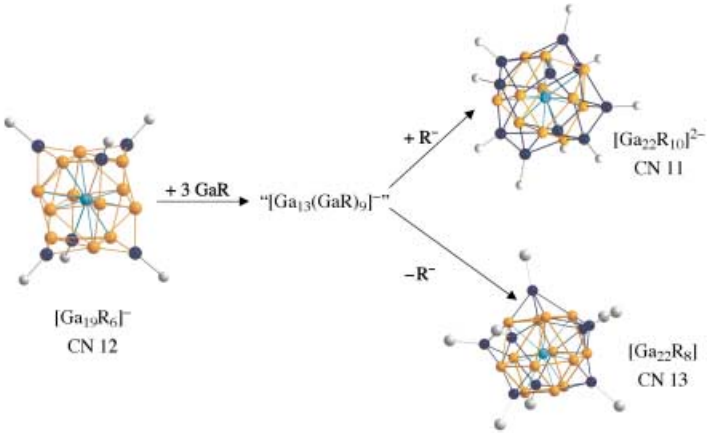

Figure 31. Variation of the coordination sphere around the central Ga atom arising from the differing steric demands of the ligands ($C(SiMe_3)_3$, $SitBu_3$, $N(SiMe_3)_2$) in the clusters **25**, **26**, and **29**.

The structure of the cluster **29** came as a surprise to us. We had long expected a further variant of a Ga_{22} cluster with a topology analogous to the $Al_{22}X_{20}$ species **6** and **7** (Section 3.2). Unfortunately despite a great deal of effort we have not been able to synthesize the analogous Ga_{22} halide. There are, however, the first indications that such a species is formed in an important primary step to the $[Ga_{84}R_{20}]^{4-}$ cluster discussed in Section 4.4.6. Recently, we succeeded in isolating a partially substituted $[Ga_{22}R_{10}Br_{10+n}]$ cluster (**30**; $n = 0-2$; $R = N(SiMe_3)_2$, Figure 32).[96] The data acquisition during the

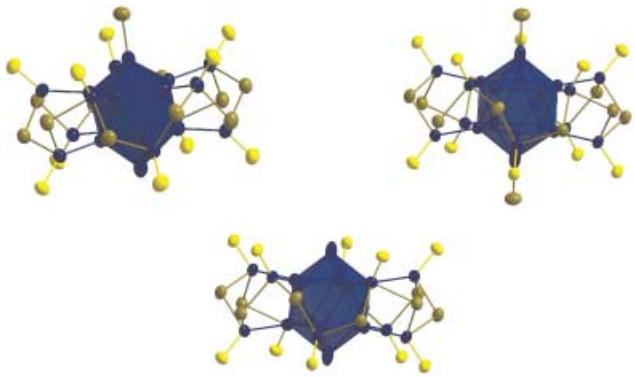

Figure 32. Preliminary molecular structure of **30** (of the $N(SiMe_3)_3$ groups only the N atoms directly bonded to the Ga atoms are shown). The central Ga_{12} icosahedron is emphasized by a polyhedral representation.

X-ray diffraction experiment and the subsequent structure analysis proved to be extremely complex for this compound, since the unit cell ($a = 40.5$; $b = 38.5$; $c = 58.8$ Å, $\alpha = \beta = \gamma = 90^\circ$) is very large. Therefore, we had to perform the X-ray diffraction experiment with the help of synchrotron radiation, and the acquired data is currently under analysis. Preliminary structure data and the graphical representations enable us to conclude that this partially substituted Ga_{22} halide is indeed an intermediate to the Ga_{84} cluster **10**. In addition, this preliminary result could be seen as an indication that a primary Ga_{22} halide analogue to the $Al_{22}X_{20}$ cluster should exist. Its existence and facile disproportionation could provide access to a modification analogous to α-boron (see Section 4.4.1).[84]

4.4.6. Ga_{84} Clusters

Under similar reaction conditions used for the synthesis of the $[Al_{77}R_{20}]^{2-}$ cluster **5** (Section 3.2), the Ga_{84} cluster $[Ga_{84}(N(SiMe_3)_2)_{20}]^{4-}$ (**10**),[97] is obtained from a metastable GaBr solution and $LiN(SiMe_3)_2$. The molecular structure of **10** is illustrated in a similar fashion to that of **5** in Figure 33.

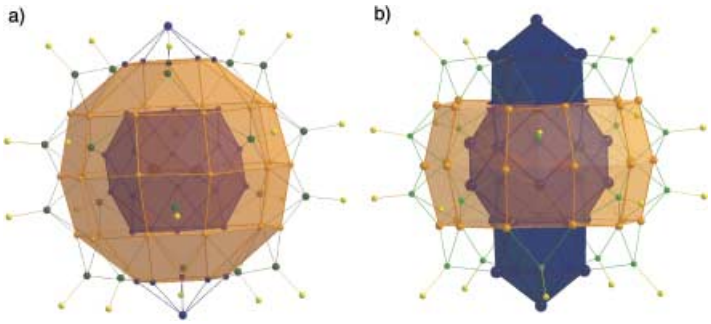

Figure 33. Molecular structure of $[Ga_{84}R_{20}]^{4-}$ (**10**; $R = N(SiMe_3)_2$ only the N atoms (yellow) directly bonded to the Ga atoms are shown). a) Layered representation analogous to the representation of the Al_{77} cluster **5** (see Figure 9b). b) Representation corresponding to the relationship of the bond lengths within the Ga_{84} cluster.

With respect to the naked metal atoms, this is the largest metalloid cluster that has ever been structurally determined by diffraction methods. The Ga_2 unit in the center of the 64 naked Ga atoms is unique in this field of chemistry (Figure 33b). The Ga_2 unit ($d(Ga{-}Ga) = 2.35$ Å), which contains a bond that is almost as short as the so-called triple Ga–Ga bond (2.32 Å) discussed in Section 4.2 and resembles the Ga_2 dumbbell unit of α-gallium. The Ga_2 unit is surrounded by a Ga_{32} shell in the form of a football with icosahedral caps (see δ-gallium (Figure 14) and $[Ga_{22}R_{10}X_{10}]$ (**30**; Figure 32). The apex and base atoms of this Ga_{32} unit are naked and are oriented towards each other in the crystal in an unusual fashion. The Ga_2Ga_{32} unit is surrounded by a "belt" of 30 Ga atoms that are also naked. Finally the entire Ga_{64} framework is protected by 20 GaR groups.

The high pseudosymmetry of the cluster molecule **10**, clearly shown in Figure 34, which resembles the approximate five- and tenfold symmetry of quasicrystals, points to molecular bonding such as that found in the fullerenes. A relationship to the recently published cadmium–gallium phases can also be perceived.[98] On the other hand the spherical layered construction (Figure 33) shows the analogy to metalloid clusters (e.g. $[Al_{77}R_{20}]^{2-}$ (**5**)), so that the bonding in **10** can be described as intermediate between the two extremes.

The arrangement of the Ga_{84} cluster in the crystal is clearly illustrated in Figure 35. The Ga_{84} clusters are lined up in "tubes". The distance between two cluster molecules that is, between the naked base and apex of gallium atoms of two clusters, is 1.3 nm, whereby two parallel oriented toluene molecules bridge the intermediate space. Although four-point measurements for electrical conductivity in the temperature range 350 to 2 K have been carried out, the mechanism of electron conductivity–**10** is a semiconductor at room temperature with a small band gap of 0.03 eV; below 7 K **10** becomes-

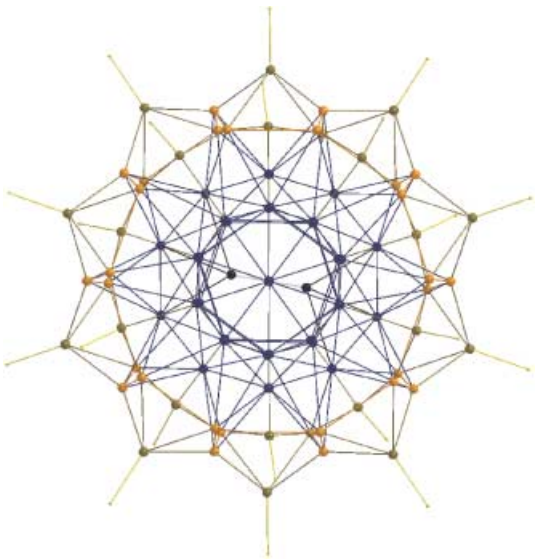

Figure 34. View of the molecular structure of **10** (of the $N(SiMe_3)_3$ groups only the N atoms directly bonded to the Ga atoms are shown) along the axis through the two naked Ga atoms.

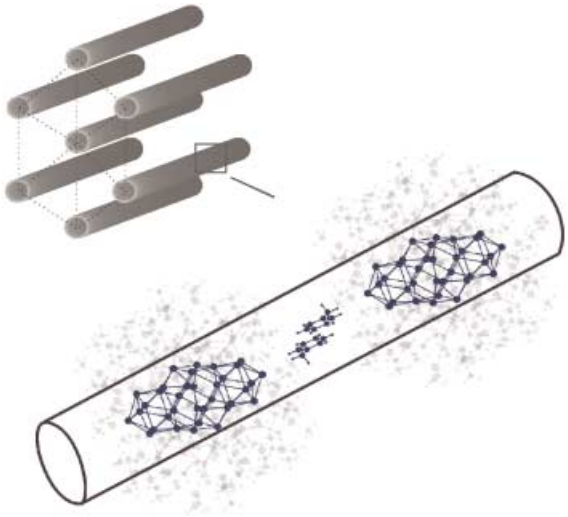

Figure 35. Molecular structure of **10** (of the $N(SiMe_3)_3$ groups only the N atoms directly bonded to the Ga atoms are shown) and arrangement of the clusters in the crystal and the two bridging toluene molecule per cluster.

superconducting at least in some ranges–cannot be conclusively explained.[99] This question is currently the subject of quantum-chemical and experimental investigations. In addition we hope with the help of synchrotron radiation to clarify the question of the possible rotation of the central Ga_2 unit and finally for the very first time for a metalloid cluster determine the electron-density distribution by experimental methods. The prerequisites for such fundamental investigations are fulfilled, since excellent crystals of **10** can be obtained in good yields.

5. Conclusions, Summary, and Outlook

Ligand-free naked metalloid clusters, for example, in molecular beams, present the first step to understanding of

the size dependence of the physical properties of metals, from nanoparticles through to the bulk phase. Quantum-chemical calculations have proven useful to supplement such investigations particularly in questions of topology.[1, 100] To obtain experimental details of the structure and to determine the physical properties of structurally known metal-atom clusters, such clusters must be protected by ligands and be available in crystalline form. With the help of such metalloid clusters it should be possible to obtain first insights into the elementary processes of dissolution and precipitation of metals from solution. To clarify such fundamental questions, however, detailed information on many metalloid clusters with different numbers of naked metal atoms in the cluster core is imperative.

The geometric structure of the M_xL_y cluster framework is the primary property according to which such clusters should be classified. Further physical data on compounds with nanostructured metalloid clusters can only be reliably interpreted when a uniform and known arrangement of the metal atoms in the cluster framework is present. Therefore, crystalline compounds of metalloid clusters are the primary prerequisite for all investigations. The next step depends on being able to isolate the individual structurally determined cluster units from the crystal lattice and then determine the physical properties of the single clusters in question. This long-term objective has been partially achieved in the gas-phase investigation of a structurally determined $[Ga_{19}R_6]^-$ cluster (**25**; $R = C(SiMe_3)_3$) in the FT mass spectrometer. Further investigations, for example, with force microscopic methods on Al and Ga clusters are currently underway.

It is amazing that such investigations have been carried out for the first time on the difficult to synthesize and difficult to handle (many compounds ignite spontaneously in air) metalloid clusters of base metals such as Al and Ga since worldwide the main emphasis of all activity in the metal atom cluster field is on the metalloid clusters of the precious metals (e.g. Au, Pt, Pd). This is understandable since these can be synthesized without great effort (e.g. in aqueous solution) and can usually be handled without the need for inert-gas techniques. The Au_{55} cluster compound[5] synthesized for the first time by Schmidt is certainly the most prominent representative of the metalloid precious-metal clusters. This Au_{55} cluster is being applied in almost all areas of chemical research concerned with functional nanostructures although there is still no detailed structural information obtained from a crystal-structure analysis. The few structure determinations on larger noble-metal clusters (see Figure 2) and all other experimental results indicate that in these cluster cores essentially the structure formed is that known from the bulk phase. This means that such precious-metal clusters can with high probability be regarded as metal particles on the nanometer scale.[101] This finding appears to be plausible since the metal–ligand interactions (e.g. Au–Cl, Au–P, Au–CO) are weaker than the metal–metal interactions in the cluster core. Changes in the ligand sphere should therefore–in contrast to the metalloid clusters of base metals–cause only minor changes in the metal atom framework.

The lack of suitable crystals of almost all metalloid noble-metal clusters on the one hand and the formation of crystals with dimensions of $1 \times 1 \times 0.5$ mm, for example, for the Ga_{84} cluster compound **10**, on the other depends apparently on different mechanisms of formation and ultimately also on the different bonding types in the two types of clusters: the noble-metal clusters are synthesized by the reduction (e.g. with BH_4^-; B_2H_6) of a noble metal salt, for example AuX_3 or PdX_2, in the presence of suitable complex builders, such as CO, PR_3. This reaction proceeds essentially spontaneously to the elementary noble metal since the activation barriers for the growth of the metalloid cluster as an intermediate are apparently very small. Fortunately there is a certain reaction step for some systems with a higher activation threshold which hinders further growth of the particular cluster species. This feature is possibly at work in the synthesis of the Au_{55} cluster so that spontaneous reaction together with very low solubility leads to the formation of tiny crystalline particles. Detailed quantum-chemical calculations could help to understand this reaction better and then possibly to influence it so that cluster growth is slowed down (e.g. by means of stronger metal–ligand bonds), to obtain larger crystals.

Apparently the method that we have developed for the disproportionation of metastable Al^I and Ga^I solutions is more suitable for the formation of crystalline compounds since the reaction conditions (temperature, donor, solvent) can be selected to influence the reactivity so that defined clusters can be isolated. The activation thresholds for the individual stages of cluster growth are very probably higher in this case than for the formation of the noble-metal clusters. This interpretation appears plausible since for the metalloid Al and Ga clusters discussed here the ligands are attached to a particular metal atom of the cluster framework by strong 2e2c bonds, which means that the formation and cleavage of such bonds, some of which are stronger than the metal–metal interactions in the cluster,[90] are associated with much higher activation thresholds than is known to be the case for ligand–noble-metal interactions. The first experimental evidence for the gas-phase reaction of a metalloid cluster ($[Ga_{19}R_6]^-$ (**25**)) indeed indicates that the GaR bonds are stronger than the Ga–Ga interactions so that a naked Ga_{13}^- cluster ion is generated in a unique fashion by the successive cleavage of GaR units.[90] Such investigations also yield the first evidence for the mechanism of dissolution of a base metal, which apparently proceeds by a different route than for the noble metals, since, for example, the Al–X bonds on the periphery of an Al_n cluster are stronger than the corresponding Au–X bonds in Au clusters.

Compared to this single piece of experimental evidence for the mechanism of dissolution of a metal, there is a multitude of aluminum and gallium clusters that can be considered as intermediates between the monohalides or their substitution products and the metal. The diversity of the clusters obtained with, in some cases, the same ligand framework enables, for the first time, an overall analysis: The drastic changes in bond lengths and coordination numbers from the cluster core to the periphery show clearly that these clusters cannot be regarded as small metal particles. For example, the two clusters of almost the same size with 69 and 77 aluminum atoms (**4** and **5**) show that small changes in the number of ligands (the ligand is identical) lead to significant changes in the cluster core. This

result means that small changes on a metal surface of dimensions of up to several nanometers could also result in geometric and electronic changes in the interior of the metal.

The diversity of observed cluster structures clearly illustrates another aspect: they generally reflect the connectivity principles that are present in the elements. Aluminum clusters predominantly show topologies of Al atoms that reflect close packing whereas gallium clusters show very different structures of the Ga frameworks corresponding to the diversity of the observed element modifications. With Ga clusters, variation of the number of ligands for the same number of total gallium atoms even allows a pseudo-nanostructured phase transition to be simulated; from $[Ga_{22}R_{10}]^{2-}$ (**29**; R = $N(SiMe_3)_2$) to $[Ga_{22}R_8]$ (**26**; R = Si*t*Bu_3). On the other hand the same ligand shell can be used to generate different packing densities in the core of the cluster: $[Ga_{18}R_8]$ (**27**; R = Si*t*Bu_3) and $[Ga_{22}R_8]$ (**26**; R = Si*t*Bu_3), so that topologies of Ga atoms result that resemble a particular normal-pressure or high-pressure modification of elemental gallium. The few results obtained so far already show that through the choice of the reaction conditions and the ligand, the cluster size and the arrangement of atoms in the cluster core can in principle be tailored, which means that nanostructured element modifications may attainable in the long-term. It could even be possible with the help of the methods developed here to synthesize elemental modifications previously known only hypothetically. For example, it is conceivable that the icosahedral subhalides (such as $Al_{22}X_{20}$ X = Cl, Br, **6** and **7**) could be linked together as building units in an analogous fashion to the linkage of fullerenes or Zintl anions,[54, 102] so that ultimately nanostructured aluminum clusters with icosahedral building units could be obtained, for example, directly by 2e2c Al–Al bonding after cleavage of Al_2X_4 (this halide has already been shown to exist during disproportionation[16a]).

Between aluminum and gallium, and also the neighboring element boron, there are great differences in the formation of clusters despite the presence of the same number of valence electrons. These differences are already obvious in the many connectivity possibilities for the atoms in the elemental forms themselves, which means that the element modifications already show that the bonding in compounds of these elements would be difficult to evaluate according to a single principle (e.g. Wade–Mingos).[67] Despite this, established rules for boron clusters can be applied to the smaller metalloid Al and Ga clusters with certain additional assumptions, as recent DFT calculations have shown.[100] In addition we have started to develop counting rules for smaller Ga and Al metalloid clusters,[103] that, however, will probably not be transferable to the larger clusters. Therefore, the first assignment principle, presented here, for the larger metalloid clusters incorporates the structures of the elements in the various modifications, which means that the metalloid or elementoid clusters are described as nanostructured element modifications.

The development of the synthesis concept described here for metalloid clusters should ultimately be capable of extension to element combinations and therefore molecular nanostructured alloys as several results on metalloid SiAl and SiGa clusters have shown.[87, 89] Such mixed clusters resemble the Zintl-type compounds.[104, 105]

Many experimental and quantum-chemical investigations are required before the final objective of a deeper understanding between the ever-increasing size of molecular cluster units and the bulk phase can be approached. It is therefore important that as many intermediates are investigated in detail with the nanoscopic methods now available. Since investigations on such sensitive samples as the Al and Ga clusters described here are associated with a large experimental effort, it cannot be expected that results will emerge quickly from the investigations currently in progress.

This research was supported by the Deutsche Forschungsgemeinschaft and the Fonds der Chemischen Industrie. STOE provided a substantial part of the costs for the color figures and the reprints for which we are very grateful.

Received: February 25, 2002 [A 520]

[1] R. Ahlrichs, S. D. Elliot, *Phys. Chem. Chem. Phys.* **1999**, *1*, 13.
[2] *Cluster and Colloids* (Ed.: G. Schmid), VCH, Weinheim, **1994**; *Metal Clusters in Chemistry* (Eds.: P. Braunstein, L. A. Oro, P. R. Raithby), Wiley-VCH, Weinheim, **1999**..
[3] A. Schnepf, G. Stößer, H. Schnöckel, *J. Am. Chem. Soc.* **2000**, *122*, 9178.
[4] F. A. Cotton, *Q. Rev. Chem. Soc.* **1966**, *20*, 397.
[5] G. Schmid, *Inorg. Synth.* **1990**, *7*, 214.
[6] A. Ceriotti, F. Demartin, G. Longoni, M. Manassero, M. Marchionna, G. Piva, M. Sansoni, *Angew. Chem.* **1985**, *97*, 708; *Angew. Chem. Int. Ed. Engl.* **1985**, *24*, 697.
[7] N. T. Tran, M. Kawano, D. R. Powell, L. F. Dahl, *J. Am. Chem. Soc.* **1998**, *120*, 10986.
[8] N. T. Tran, D. R. Powell, L. F. Dahl, *Angew. Chem.* **2000**, *112*, 4287; *Angew. Chem. Int. Ed.* **2000**, *39*, 4121.
[9] A. Ecker, E. Weckert, H. Schnöckel, *Nature* **1997**, *387*, 379.
[10] W. Uhl, *Z. Naturforsch. B* **1988**, *43*, 1113.
[11] W. Uhl, W. Hiller, M. Layh, W. Schwarz, *Angew. Chem.* **1992**, *104*, 1378; *Angew. Chem. Int. Ed. Engl.* **1992**, *31*, 1364.
[12] S. Schulz, H. W. Roesky, H. J. Koch, G. M. Sheldrick, D. Stalke, A. Kuhn, *Angew. Chem.* **1993**, *105*, 1828; *Angew. Chem. Int. Ed. Engl.* **1993**, *32*, 1729.
[13] N. Wiberg, *Coord. Chem. Rev.* **1997**, *163*, 217.
[14] G. Linti, *J. Organomet. Chem.* **1996**, *520*, 107.
[15] M. L. H. Green, P. Mountford, G. Smout, S. Speel, *Polyhedron* **1990**, *22*, 2763.
[16] a) C. Dohmeier, D. Loos, H. Schnöckel, *Angew. Chem.* **1996**, *108*, 141; *Angew. Chem. Int. Ed. Engl.* **1996**, *35*, 129; b) "Group 13 Chemistry" H. Schnöckel, A. Schnepf, *ACS Symp. Ser.* **2002**, *822*, 154; c) H. Schnöckel, H. Köhnlein, *Polyhedron* **2002**, 489; d) G. Linti, H. Schnöckel, *Coord. Chem. Rev.* **2000**, *206–207*, 285.
[17] M. Tacke, H. Schnöckel, *Inorg. Chem.* **1989**, *28*, 2895.
[18] M. W. Chase, Jr., C. A. Davies, J. R. Downey, Jr., D. J. Frurip, R. A. McDonal, A. N. Syverend, *JANNAF-Thermodynamical Tables*, *3rd ed.*, American Chemical Society, American Institute of Physics, US National Bureau of Standards, Midland, MI, **1985**.
[19] H. Schäfer, *Chemische Transportreaktionen*, Verlag Chemie, Weinheim, **1962**; L. Troost, P. Hautefeuille, *C. R. Hebd. Seances Acad. Sci.* **1885**, *100*, 1220; W. Klemm, E. Voss, K. Geiersberger, *Z. Anorg. Allg. Chem.* **1948**, *256*, 15, 24.
[20] R. Ahlrichs, L. Zhengyan, H. Schnöckel, *Z. Anorg. Allg. Chem.* **1984**, *519*, 155.
[21] H. Schnöckel, *J. Mol. Struct.* **1978**, *50*, 275.
[22] J. Bahlo, H.-J. Himmel, H. Schnöckel, *Angew. Chem.* **2001**, *113*, 4820; *Angew. Chem. Int. Ed.* **2001**, *40*, 4696.
[23] H. Schnöckel, A. Schnepf, *Adv. Organomet. Chem.* **2001**, *47*, 235.

[24] M. Mocker, C. Robl, H. Schnöckel, *Angew. Chem.* **1994**, *106*, 1860; *Angew. Chem. Int. Ed. Engl.* **1994**, *33*, 1754; A. Ecker, H. Schnöckel, *Z. Anorg. Allg. Chem.* **1996**, *622*, 149.

[25] C. U. Doriat, E. Baum, A. Ecker, H. Schnöckel, *Angew. Chem.* **1997**, *109*, 2057; *Angew. Chem. Int. Ed. Engl.* **1997**, *36*, 1969.

[26] C. Klemp, M. Bruns, J. Gauss, U. Häussermann, G. Stößer, L. van Wühlen, M. Jansen, H. Schnöckel, *J. Am. Chem. Soc.* **2001**, *123*, 9099.

[27] C. Klemp, R. Köppe, E. Weckert, H. Schnöckel, *Angew. Chem.* **1999**, *111*, 1852; *Angew. Chem. Int. Ed.* **1999**, *38*, 1740.

[28] H. Schnöckel, C. Klemp in *Inorganic Chemistry Highlights* (Eds.: G. Meyer, D. Naumann, L. Wesemann), Wiley-VCH, **2002**, p. 245.

[29] A. Haaland, K.-G. Martinsen, H. V. Volden, D. Loos, H. Schnöckel, *Acta Chem. Scand.* **1994**, *48*, 172; D. Loos, E. Baum, A. Ecker, H. Schnöckel, A. J. Downs, *Angew. Chem.* **1997**, *109*, 854; *Angew. Chem. Int. Ed. Engl.* **1997**, *36*, 860; P. Jutzi, B. Neumann, G. Reumann, H.-G. Stammler, *Organometallics* **1998**, *17*, 1305.

[30] D. Loos, H. Schnöckel, J. Gauss, U. Schneider, *Angew. Chem.* **1992**, *104*, 1376; *Angew. Chem. Int. Ed. Engl.* **1992**, *31*, 1362.

[31] J. Gauss, U. Schneider, R. Ahlrichs, C. Dohmeier, H. Schnöckel, *J. Am. Chem. Soc.* **1993**, *115*, 2402.

[32] A. Schnepf, R. Köppe, H. Schnöckel, *Angew. Chem.* **2001**, *113*, 1287; *Angew. Chem. Int. Ed.* **2001**, *40*, 1241.

[33] C. Dohmeier, C. Robl, M. Tacke, H. Schnöckel, *Angew. Chem.* **1991**, *103*, 594; *Angew. Chem. Int. Ed. Engl.* **1991**, *30*, 564; the alternative classical synthesis was published more than two years later.[12]

[34] A. Purath, R. Köppe, H. Schnöckel, *Angew. Chem.* **1999**, *111*, 3114; *Angew. Chem. Int. Ed.* **1999**, *38*, 2926.

[35] A. Purath, R. Köppe, H. Schnöckel, *Chem. Commun.* **1999**, 1933.

[36] H. Köhnlein, A. Purath, C. Klemp, E. Baum, I. Krossing, G. Stößer, H. Schnöckel, *Inorg. Chem.* **2001**, *40*, 4830.

[37] H. Köhnlein, G. Stößer, E. Baum, E. Möllhausen, U. Huniar, H. Schnöckel, *Angew. Chem.* **2000**, *112*, 828; *Angew. Chem. Int. Ed.* **2000**, *39*, 799.

[38] The structure of **2** is identical to that of a $[In_{12}R_8]$ species[83] ($R = Si{t}Bu_3$), whereby the bulkier $Si{t}Bu_3$ group surrounds the In_{12} core as opposed to the $N(SiMe_3)_2$ ligands of **2**. In contrast to the typical topology for metals that form close-packed structures in the elemental form, a distorted icosahedral framework of 12 Ga atoms is observed for $[Ga_{12}R_{10}]^{2-}$ (**21**, i.e. $[Ga_{12}R_8]$, after cleavage of $2\,R^-$ groups, see Section 4.4.1).

[39] For the corresponding hypothetical Ga_{14} compound, however, according to quantum-chemical calculations the polyhedral structure is favored over the "wheel-rim" structure; H. Köhnlein, *Dissertation*, Karlsruhe, **2001**.

[40] J.-Y. Yi, *Phys. Rev. B* **2000**, *61*, 7277.

[41] X. G. Gong, D. Y. Sun, X.-Q. Wang, *Phys. Rev. B* **2000**, *62*, 15413.

[42] J. A. Morrison, *Chem. Rev.* **1991**, *91*, 35; W. Hönle, Y. Grin, A. Burkhardt, U. Wedig, M. Schultheiss, H. G. von Schnering, R. Keller, H. Binder, *J. Solid. State Chem.* **1997**, *133*, 59.

[43] B. F. Decker, J. S. Kasper, *Acta Crystallogr.* **1959**, *12*, 503.

[44] Both procedures were initially tested on the less sensitive $(AlCp^*)_4$.[26] It was experimentally demonstrated for the first time that the Al atoms in this Al^I organic compound can be assigned an oxidation state that lies in-between that of the metal and classical Al^{III} compounds (e.g. Al_2O_3).

[45] F. Laves, *Naturwissenschaften* **1932**, *20*, 472.

[46] L. Bosio, A. Defrain, *Acta Crystallogr. Sect B* **1969**, *25*, 995.

[47] L. Bosio, H. Curien, M. Dupont, A. Rimsky, *Acta Crystallogr. Sect B* **1972**, *28*, 1974.

[48] L. Bosio, H. Curien, M. Dupont, A. Rimsky, *Acta Crystallogr. Sect B* **1973**, *29*, 367.

[49] a) L. Bosio, *J. Chem. Phys.* **1978**, *68*, 1221; b) O. Schulte, W. B. Holzapfel, *Phys. Rev. B* **1997**, *55*, 8122; K. Takemure, K. Kobayashi, M. Arai, *Phys. Rev. B* **1998**, *58*, 2482.

[50] H. von Schnering, R. Nesper, *Acta Chem. Scand.* **1991**, *45*, 870; U. Häusermann, S. Simak, I. Abrikosov, S. Lidin, *Chemistry* **1997**, *3*, 904; X. G. Gong, G. Chiarotti, M. Parinello, E. Tosatti, *Phys. Rev. B* **1991**, *43*, 14277.

[51] We recently summarized all Ga_n clusters with more than two Ga atoms in a table.[93,23]

[52] $Br_2Ga\text{-}GaBr_2 \cdot 2L$ compounds were synthesized earlier a) J. C. Beamish, R. W. H. Small, I. J. Worall, *Inorg. Chem.* **1979**, *18*, 220; b) K. L. Brown, D. Hall, *J. Chem. Soc. Dalton Trans.* **1973**, 1843; H. Schmidbaur, *Angew. Chem.* **1985**, *97*, 893; *Angew. Chem. Int. Ed. Engl.* **1985**, *24*, 893; c) G. Gerlach, W. Hönle, A. Simon, *Z. Anorg. Allg. Chem.* **1982**, *486*, 7 and in α-Ga there are particularly short Ga–Ga bonds (2.45 Å), as a result of which the α-modification has been designated a molecular metal.[50]

[53] W. Uhl, M. Layh, T. Hildebrand, *J. Organomet. Chem.* **1989**, *364*, 289.

[54] T. F. Fässler, *Angew. Chem.* **2001**, *113*, 4289; *Angew. Chem. Int. Ed.* **2001**, *40*, 4161.

[55] Y. Xie, R. S. Grev, J. Ga, H. F. Schäfer III, P. von R. Schleyer, J. Su, X.-W. Li, G. H. Robinson, *J. Am. Chem. Soc.* **1998**, *120*, 3773; N. Takagi, M. W. Schmidt, S. Nagase, *Organometallics* **2001**, *20*, 1646; A. J. Bridgeman, L. R. Ireland, *Polyhedron* **2001**, 2841.

[56] J. Su, X.-W. Li, R. C. Crittendon, G. H. Robinson, *J. Am. Chem. Soc.* **1997**, *119*, 5471.

[57] With the help of the metastable AlX solutions (Section 2.1) it should be possible in principle, by means of metathesis with larger ligands, such as the substituted supermesityl groups $t{Bu}_3C_6H_2$ used by Robinson and Power, to synthesize the corresponding aluminum compounds such as $[RAlAlR]^{2-}$. However, all previous attempts, also those in collaboration with Power and co-workers, have failed mainly because of the lack of crystallization of the required product, since the reaction solutions usually contain many compounds that cannot be separated.

[58] T. Pott, P. Jutzi, W. Schoeller, A. Stammler, H.-G. Stammler, *Organometallics* **2001**, *20*, 5492.

[59] R. Köppe, H. Schnöckel, *Z. Anorg. Allg. Chem.* **2000**, *626*, 1095; G. Linti, H. Schnöckel, *Coord. Chem. Rev.* **2000**, *206*, 285.

[60] H.-J. Himmel, H. Schnöckel, *Chemistry*, **2002**, *8*, 2397.

[61] Since for the heavier main-group elements it appears that some of the bonding electrons are located in orbitals that show predominantly AO character, we have modified the designation as follows: double or triple bonds should be designated as $(4-x)$e2c or $(6-x)$e2c bonds. All bonds can be described in this fashion, for example, x is a 0 for C_2H_4 and 4 for Ga_2H_2.[60]

[62] X.-W. Li, W. T. Pennington, G. H. Robinson, *J. Am. Chem. Soc.* **1995**, *117*, 7578; X.-W. Li, Y. Xie, P. R. Schreiner, K. D. Gripper, R. C. Crittendon, C. F. Campana, H. F. Schaefer, G. H. Robinson, *Organometallics* **1996**, *15*, 3798.

[63] The recently described ring-shaped $[Ga_3R_4]$ ($R =$ supersilyl) species with a mean oxidation state of $+1.3$ cannot be assigned in this way. N. Wiberg, T. Blank, K. Amelunxen, H. Nöth, J. Knizek, T. Habereder, W. Kaim, M. Wanner, *Eur. J. Inorg. Chem.* **2001**, *7*, 1719.

[64] B. Twanley, P. P. Power, *Angew. Chem.* **2000**, *112*, 3643; *Angew. Chem. Int. Ed.* **2000**, *39*, 3500.

[65] A. I. Boldyrev, A. E. Kuznetsov, *Inorg. Chem.* **2002**, *41*, 532.

[66] G. Linti, *J. Organomet. Chem.* **1996**, *520*, 107; G. Linti, A. Rodig, *Chem. Commun.* **2000**, 127; N. Wiberg, K. Amelunxen, H.-W. Lerner, H. Nöth, W. Ponikwar, H. Schwenk, *J. Organomet. Chem.* **1999**, *574*, 246.

[67] K. Wade, *Adv. Inorg. Chem. Radiochem.* **1976**, *18*, 1; R. W. Rudolph, *Acc. Chem. Res.* **1976**, *9*, 446; R. E. Williams, *Adv. Inorg. Chem. Radiochem.* **1976**, *18*, 67; D. M. P. Mingos, *Nature* **1972**, *336*, 99.

[68] N. Wiberg, T. Blank, M. Westerhausen, S. Schneiderbauer, H. Schnöckel, I. Krossing, A. Schnepf, *Eur. J. Inorg. Chem.* **2002**, 351.

[69] R. J. Wehmschulte, P. P. Power, *Angew. Chem.* **1998**, *110*, 3344; *Angew. Chem. Int. Ed.* **1998**, *37*, 3154.

[70] D. Loos, H. Schnöckel, D. Fenske, *Angew. Chem.* **1993**, *105*, 1124; *Angew. Chem. Int. Ed. Engl.* **1993**, *32*, 1059.

[71] C. Klemp, G. Stößer, I. Krossing, H. Schnöckel, *Angew. Chem.* **2000**, *112*, 3834; *Angew. Chem. Int. Ed.* **2000**, *39*, 3691.

[72] A. Donchev, A. Schnepf, E. Baum, G. Stößer, H. Schnöckel, *Z. Anorg. Allg. Chem.* **2001**, *628*, 157.

[73] J. Thesing, J. Baumeister, W. Preetz, D. Thiery, H. G. von Schnering, *Z. Naturforsch. B* **1991**, *46*, 800; A. Heinrich, H.-L. Keller, W. Preetz, *Z. Naturforsch. B* **1990**, *45*, 184; $B_6X_6^-$: V. Lorensen, W. Preetz, F. Baumann, W. Kaim, *Inorg. Chem.* **1998**, *37*, 4011.

[74] C. Dohmeier, M. Mocker, H. Schnöckel, A. Lötz, U. Schneider, R. Ahlrichs, *Angew. Chem.* **1993**, *105*, 1491; *Angew. Chem. Int. Ed. Engl.* **1993**, *32*, 1428.

[75] N. Wiberg, T. Blank, H. Nöth, M. Suter, M. Warchold, *Eur. J. Inorg. Chem.*, in press.

[76] A recently described $[In_8R_6]$ cluster (R = supersilyl) contains another variant of a E_8-triel framework in which only two diagonally arranged In atoms of a distorted cube are not attached to ligands. N. Wiberg, T. Blank, A. Purath, G. Stößer, H. Schnöckel, *Angew. Chem.* **1999**, *111*, 2745; *Angew. Chem. Int. Ed.* **1999**, *38*, 2563.
[77] A. Schnepf, G. Stößer, H. Schnöckel, *Z. Anorg. Allg. Chem.* **2000**, *626*, 1676.
[78] W. Uhl, L. Cuypers, K. Harms, W. Kaim, M. Wanner, R. Winter, R. Koch, W. Saak, *Angew. Chem.* **2001**, *113*, 589; *Angew. Chem. Int. Ed.* **2001**, *40*, 566.
[79] L. M. McKee, Z.-X. Wang, P. von R. Schleyer, *J. Am. Chem. Soc.* **2000**, *122*, 4781; H. Binder, R. Kellner, K. Vaas, M. Hein, F. Baumann, M. Wanner, R. Winter, W. Kaim, W. Hönle, Y. Grin, U. Wedig, M. Schultheiß, R. K. Kremer, H. G. von Schnering, O. Groeger, G. Engelhardt, *Z. Anorg. Allg. Chem.* **1999**, *625*, 1059.
[80] W. Köstler, G. Linti, *Angew. Chem.* **1997**, *109*, 2758; *Angew. Chem. Int. Ed. Engl.* **1997**, *36*, 2644.
[81] W. Hiller, K.-W. Klinkhammer, W. Uhl, J. Wagner, *Angew. Chem.* **1991**, *103*, 182; *Angew. Chem. Int. Ed. Engl.* **1991**, *30*, 179.
[82] A. Schnepf, G. Stößer, R. Köppe, H. Schnöckel, *Angew. Chem.* **2000**, *112*, 1709; *Angew. Chem. Int. Ed.* **2000**, *39*, 1637.
[83] N. Wiberg, T. Blank, H. Nöth, W. Ponikwar, *Angew. Chem.* **1999**, *111*, 887; *Angew. Chem. Int. Ed.* **1999**, *38*, 839.
[84] U. Häussermann, S. I. Simiak, R. Ahuja, B. Johansson, personal communication.
[85] M. Kehrwald, W. Köstler, A. Rodig, G. Linti, T. Blank, N. Wiberg, *Organometallics* **2001**, *20*, 860.
[86] J. Steiner, E. Baum, G. Linti, H. Schnöckel, unpublished results.
[87] A. Purath, C. Dohmeier, A. Ecker, R. Köppe, H. Krautscheid, H. Schnöckel, R. Ahlrichs, C. Stoermer, J. Friedrich, P. Jutzi, *J. Am. Chem. Soc.* **2000**, *122*, 6955.
[88] A comparable cluster expansion in the direction of a centered Ga structure is observed for the $[Ga_{26}R_8]^{2-}$ cluster **28** in which the cluster core of 18 naked Ga atoms is shielded by the same type of ligand as in **24′** and **23**.
[89] K. Weiss, R. Köppe, H. Schnöckel, *Int. J. Mass Spectrom.* **2002**, *214*, 383.
[90] K. Weiss, R. Köppe, H. Schnöckel, unpublished results.
[91] A. Schnepf, E. Weckert, G. Linti, H. Schnöckel, *Angew. Chem.* **1999**, *111*, 3578; *Angew. Chem. Int. Ed.* **1999**, *38*, 3381.
[92] G. Linti, G, A. Rodig, *Chem. Commun.* **2000**, 127.
[93] A. Donchev, A. Schnepf, G. Stößer, E. Baum, H. Schnöckel, T. Blank, N. Wiberg, *Chem. Eur. J.* **2001**, *7*, 3348.
[94] A. Rodig, G. Linti, *Angew. Chem.* **2000**, *112*, 3076; *Angew. Chem. Int. Ed.* **2000**, *39*, 2952.
[95] A. Schnepf, G. Stößer, H. Schnöckel, *Angew. Chem.* **2002**, *114*, 1959; *Angew. Chem. Int. Ed.* **2002**, *41*, 1882.
[96] A. Schnepf, H. Schnöckel, unpublished results.
[97] A. Schnepf, H. Schnöckel, *Angew. Chem.* **2001**, *113*, 734; *Angew. Chem. Int. Ed.* **2001**, *40*, 711.
[98] C. P. Gomez, S. Lidin, *Angew. Chem.* **2001**, *113*, 4161; *Angew. Chem. Int. Ed.* **2001**, *40*, 4037.
[99] J. Hagel, M. T. Kelemen, G. Fischer, B. Pilawa, J. Wosnitza, E. Dormann, H. von Löhneysen, A. Schnepf, H. Schnöckel, U. Neisel, J. Beck, *J. Low Temp. Phys.*, accepted.
[100] W. H. Lam, Z. Lin, *Polyhedron* **2002**, *21*, 503.
[101] Since the energy difference between a cubooctahedral and icosahedral environment of the central metal atom is small, both possibilities are often observed or discussed. J. W. A. van der Velden, F. A. Vollenbroek, J. J. Bour, P. I. Beursken, J. M. M. Smits, W. P. Bosman, *Rec. J. R. Neth. Chem. Soc.* **1981**, *100*, 148; B. K. Teo, X. Shi, H. Zhang, *J. Am. Chem. Soc.* **1992**, *114*, 2743.[5]
[102] A similar connectivity for nanoscale molybdate clusters was recently described by Müller et al.: A. Müller, S. K. Das, M. O. Talismanova, H. Bögge, P. Kögerler, M. Schmidtmann, S. S. Talismanov, M. Luban, E. Krickemeyer, *Angew. Chem.* **2002**, *114*, 599; *Angew. Chem. Int. Ed.* **2002**, *41*, 579.
[103] We have been able to demonstrate that in E_nX_{n+y} subhalides or in the partially substituted clusters $n - ½y$ molecular orbitals for E–E bonding are available, which means that 2e2c bonds are only available for $y \leq 0$ (e.g. in ring-shaped Al_4X_4).[26] C. Klemp, *Dissertation*, Karlsruhe **2000**.
[104] J. D. Corbett, *Angew. Chem.* **2000**, *112*, 682; *Angew. Chem. Int. Ed.* **2000**, *39*, 692.
[105] Although there are many cases of topological similarity between the Zintl clusters and the metalloid clusters described here–e.g. in the fullerene-type In_{74} cluster of the $Na_{96}In_{97}Ni_2$ phase[106]–the differences cannot be overlooked: Zintl-type clusters usually carry a large negative charge (e.g. Tl_{13}^{10-} in $Na_4K_6Tl_{13}$),[107] and therefore can only be stabilized by the lattice energy from a sea of positive charge. The preparation conditions of these phases show that the great "electron hunger" of Group 13 elements can only be satisfied by the strong reductive strength of the alkali metals, and as a result the mean oxidation state for all Zintl-type clusters is negative which is why these clusters are to be found above the Fermi level. In contrast the mean oxidation state of all the metalloid Al and Ga clusters described here is positive which means these are compounds that are on the way from the oxidized species (here Al^{1+}, Ga^{1+}) to the metal and the HOMOs of these molecular clusters lie below the Fermi level.
[106] S. C. Sevor, J. D. Corbett, *Science* **1993**, *262*, 880.
[107] G. Cordier, V. Müller, *Z. Naturforsch. B* **1994**, *49*, 935; Z.-C. Dong, J. D. Corbett, *J. Am. Chem. Soc.* **1995**, *117*, 6447.
[108] Z.-C. Dong, J. D. Corbett, *J. Am. Chem. Soc.* **1995**, *117*, 6447.